

AN ALGEBRAIC DESCRIPTION OF SCREW DISLOCATIONS IN SC AND BCC CRYSTAL LATTICES

HIROYASU HAMADA, SHIGEKI MATSUTANI, JUNICHI NAKAGAWA, OSAMU SAEKI,
AND MASAOKI UESAKA

ABSTRACT. We give an algebraic description of screw dislocations in a crystal, especially simple cubic (SC) and body centered cubic (BCC) crystals, using free abelian groups and fibering structures. We also show that the strain energy of a screw dislocation based on the spring model is expressed by the Epstein-Hurwitz zeta function approximately. Crystal lattice and screw dislocation and topological defect and monodromy and group ring of abelian group and dislocation energy and Epstein-Hurwitz zeta function

1. INTRODUCTION

Mathematical descriptions of dislocations in crystal lattices have been studied extensively in the framework of differential geometry or continuum geometry [A1, A2, KE, Kon, N]. However, crystal structures are usually given as discrete geometry. In fact, a crystal lattice is governed by a discrete group such as free abelian group [CS, Koh, S]. An abelian group and its group ring provide fruitful mathematical tools, e.g., abelian varieties, theta functions, and so on. On the other hand, the continuum geometric nature of dislocations in the euclidean space cannot be represented well as long as we use the ordinary algebraic expressions.

In this article, we give algebraic descriptions of screw dislocations in the simple cubic (SC) and the body centered cubic (BCC) crystals in terms of certain “fibrations” involving group rings. Using such fibering structures, we describe the continuum geometric property embedded in the euclidean space, whereas the algebraic structures involving group rings enable us to describe the discrete nature of the crystal lattices. More precisely, we first describe the screw dislocations in continuum picture and then we use algebraic structures of lattices to embed their “discrete dislocations” in the continuum description. Our key idea is to use certain sections of S^1 -bundles to control the behavior of dislocations.

We also show that the strain energy of a screw dislocation based on the spring model is expressed by the Epstein-Hurwitz zeta function [Ep, El] approximately. This will be shown by using our algebraic description of a screw dislocation.

It should be noted that the results presented in this article arose in our attempt to solve the following problems proposed in the Study Group Workshop at Kyushu University and the University of Tokyo, held during July 29–Aug 4, 2015 [O].

- (1) To find a proper mathematical description of a screw dislocation in the BCC lattice.

- (2) To find a proper mathematical description of the strain energy of a screw dislocation in the BCC lattice.

The present article is organized as follows. In Section 2, we first introduce certain fibering structures over the plane involving the celebrated exact sequence

$$0 \rightarrow \mathbb{Z} \rightarrow \mathbb{R} \rightarrow U(1) \rightarrow 1,$$

which will be essential in this article. Then, we will describe screw dislocations in continuum picture, in which certain covering spaces of a punctured complex plane will play important roles. By using certain path spaces, we clarify the covering structures of screw dislocations in Remark 2.4 and Proposition 2.6. In Section 3, we first explain the algebraic structure of the SC lattice as a free abelian group. Then, we consider the fibering structure of the SC lattice in terms of the associated group ring and its quotient. Using these descriptions, we will describe the screw dislocations in the SC lattice in Propositions 3.6 and 3.8 so that they are embedded in the continuum picture given in Section 2. In Section 4, we first explain the fibering structure of the SC lattice in a diagonal direction, using group ring structures. Then, we explain similar structures for the BCC lattice. Finally, screw dislocations in the BCC lattice will be described using all these algebraic materials in Propositions 4.14 and 4.15. Section 5 is devoted to the computation of the strain or elastic energy of a single screw dislocation in the SC lattice. In Theorem 5.2, the elastic energy of the dislocation corresponding to a bounded annular region is expressed in terms of the truncated Epstein-Hurwitz zeta function [Ep, El] approximately. In Section 6, we summarize and discuss our results from various viewpoints. In particular, in Section 6.2, we provide explanations from physical points of view so that even the readers who may not be familiar with mathematical tools can understand our results. Finally, in the appendix, we show that the total elastic energy for two parallel screw dislocations with opposite directions does not diverge for unbounded regions, both in the continuum picture and in the discrete picture.

1.1. Notations and Conventions. Throughout the article, we distinguish the euclidean space \mathbb{E} from the real vector space \mathbb{R} : in particular, \mathbb{R} is endowed with an algebraic structure, while \mathbb{E} is not. We often identify the 2-dimensional euclidean space \mathbb{E}^2 with the complex plane \mathbb{C} . The group $U(1)$ acts on the set S^1 simply transitively. Given a fiber bundle $\mathcal{F} \rightarrow \mathcal{M}$ over a base space \mathcal{M} , we denote the set of all continuous sections $f : \mathcal{M} \rightarrow \mathcal{F}$ by $\Gamma(\mathcal{M}, \mathcal{F})$.

2. SCREW DISLOCATIONS IN CONTINUUM PICTURE

Let us consider the exact sequence of groups (see [B])

$$(2.1) \quad 0 \longrightarrow \mathbb{Z} \xrightarrow{\iota} \mathbb{R} \xrightarrow{\exp 2\pi\sqrt{-1}} U(1) \longrightarrow 1,$$

where \mathbb{Z} and \mathbb{R} are additive groups, $U(1)$ is a multiplicative group, $\iota(n) = n$ for $n \in \mathbb{Z}$, and $(\exp 2\pi\sqrt{-1})(x) = \exp(2\pi\sqrt{-1}x)$ for $x \in \mathbb{R}$. Throughout this section, we fix $d > 0$.

For $\delta \in \mathbb{R}$, we have the “shifts”

$$\begin{aligned} \tilde{\iota}_\delta : \mathbb{R} &\rightarrow \mathbb{E} \text{ defined by } x \mapsto d \cdot x + \delta, \quad x \in \mathbb{R}, \text{ and} \\ \iota_\delta : \text{U}(1) &\rightarrow S^1 \text{ defined by } \exp(\sqrt{-1}\theta) \mapsto \exp \sqrt{-1}(\theta + 2\pi\delta/d), \quad \theta \in \mathbb{R}, \end{aligned}$$

such that the following diagram is commutative:

$$\begin{array}{ccccccc} & & & \mathbb{E} & \xrightarrow{\psi} & S^1 & \\ & & \nearrow \varphi_\delta & \uparrow \tilde{\iota}_\delta & & \uparrow \iota_\delta & \\ 0 & \longrightarrow & \mathbb{Z} & \xrightarrow{\iota} & \mathbb{R} & \xrightarrow{\exp 2\pi\sqrt{-1}} & \text{U}(1) \longrightarrow 1, \end{array}$$

where $\psi(y) = \exp(2\pi\sqrt{-1}y/d)$, $y \in \mathbb{R}$, and $\varphi_\delta = \tilde{\iota}_\delta \circ \iota$. Note that for the sequence of maps

$$\mathbb{Z} \xrightarrow{\varphi_\delta} \mathbb{E} \xrightarrow{\psi} S^1,$$

we have

$$(2.2) \quad \varphi_\delta(\mathbb{Z}) = \psi^{-1}(\exp(2\pi\sqrt{-1}\delta/d)),$$

which is a consequence of the exactness of (2.1).

2.1. Fiberling Structures of Crystals in Continuum Picture. Let us consider the 2-dimensional euclidean space \mathbb{E}^2 and some trivial bundles over \mathbb{E}^2 ; \mathbb{Z} -bundle $\pi_{\mathbb{Z}} : \mathbb{Z}_{\mathbb{E}^2} \rightarrow \mathbb{E}^2$, \mathbb{E} -bundle $\pi_{\mathbb{E}} : \mathbb{E}_{\mathbb{E}^2} \rightarrow \mathbb{E}^2$ and S^1 -bundle $\pi_{S^1} : S^1_{\mathbb{E}^2} \rightarrow \mathbb{E}^2$. We consider the bundle maps $\widehat{\varphi}_\delta$ and $\widehat{\psi}$,

$$(2.3) \quad \mathbb{Z}_{\mathbb{E}^2} \xrightarrow{\widehat{\varphi}_\delta} \mathbb{E}_{\mathbb{E}^2} \xrightarrow{\widehat{\psi}} S^1_{\mathbb{E}^2},$$

naturally induced by φ_δ and ψ , respectively.

Note that $\mathbb{Z}_{\mathbb{E}^2} = \mathbb{Z} \times \mathbb{E}^2$ is a covering space of \mathbb{E}^2 and that $\mathbb{E}_{\mathbb{E}^2}$ is identified with $\mathbb{E}^3 = \mathbb{E} \times \mathbb{E}^2$. We sometimes use such identifications.

In the following, we often identify \mathbb{E}^2 with the complex plane \mathbb{C} . For $\gamma \in S^1$, let us consider the global constant section $\sigma_\gamma \in \Gamma(\mathbb{E}^2, S^1_{\mathbb{E}^2})$ of $S^1_{\mathbb{E}^2}$ defined by

$$\sigma_\gamma(z) = (\gamma, z) \in S^1_{\mathbb{E}^2} = S^1 \times \mathbb{E}^2$$

for $z \in \mathbb{E}^2 = \mathbb{C}$. The following lemma is straightforward by virtue of (2.2).

Lemma 2.1. *For $\gamma = \exp(2\pi\sqrt{-1}\delta/d)$, we have*

$$\mathbb{Z}_{\mathbb{E}^2, \gamma} = \widehat{\varphi}_\delta(\mathbb{Z}_{\mathbb{E}^2}),$$

where

$$\mathbb{Z}_{\mathbb{E}^2, \gamma} := \widehat{\psi}^{-1}(\sigma_\gamma(\mathbb{E}^2)) \subset \mathbb{E}^3.$$

2.2. Single Screw Dislocation in Continuum Picture. For $z_0 \in \mathbb{E}^2 = \mathbb{C}$, let us consider the trivial bundles $\mathbb{E}_{\mathbb{E}^2 \setminus \{z_0\}}$ and $S^1_{\mathbb{E}^2 \setminus \{z_0\}}$ over $\mathbb{E}^2 \setminus \{z_0\}$ as in the previous subsection. For $\gamma \in S^1$, let us consider the section $\sigma_{z_0, \gamma} \in \Gamma(\mathbb{E}^2 \setminus \{z_0\}, S^1_{\mathbb{E}^2 \setminus \{z_0\}})$ defined by

$$\sigma_{z_0, \gamma}(z) = \left(\gamma \frac{z - z_0}{|z - z_0|}, z \right) \text{ for } z \in \mathbb{E}^2 \setminus \{z_0\} = \mathbb{C} \setminus \{z_0\}.$$

We set

$$\mathbb{Z}_{\mathbb{E}^2 \setminus \{z_0\}, \gamma} := \widehat{\psi}^{-1}(\sigma_{z_0, \gamma}(\mathbb{E}^2 \setminus \{z_0\})) \subset \mathbb{E}_{\mathbb{E}^2 \setminus \{z_0\}} \subset \mathbb{E}^3$$

and let $\pi_{z_0, \gamma} : \mathbb{Z}_{\mathbb{E}^2 \setminus \{z_0\}, \gamma} \rightarrow \mathbb{E}^2 \setminus \{z_0\}$ be defined by $\pi_{z_0, \gamma} = \pi_{\mathbb{E}}|_{\mathbb{Z}_{\mathbb{E}^2 \setminus \{z_0\}, \gamma}}$.

Lemma 2.2. *The map $\pi_{z_0, \gamma} : \mathbb{Z}_{\mathbb{E}^2 \setminus \{z_0\}, \gamma} \rightarrow \mathbb{E}^2 \setminus \{z_0\}$ defines a universal covering of $\mathbb{E}^2 \setminus \{z_0\}$.*

Proof. Over each point of \mathbb{E}^2 , $\widehat{\psi}$ is a covering map and it is trivial as a family of covering maps. Therefore, we see that $\pi_{z_0, \gamma}$ defines a covering map.

Furthermore, $\mathbb{Z}_{\mathbb{E}^2 \setminus \{z_0\}, \gamma}$ is path-wise connected. This is seen as follows. Let us take arbitrary two points x_1 and x_2 . Then $\pi_{z_0, \gamma}(x_1)$ and $\pi_{z_0, \gamma}(x_2)$ are connected by a path in $\mathbb{E}^2 \setminus \{z_0\}$. By lifting such a path, we see that x_1 is connected in $\mathbb{Z}_{\mathbb{E}^2 \setminus \{z_0\}, \gamma}$ to a point x'_1 such that $\pi_{z_0, \gamma}(x'_1) = \pi_{z_0, \gamma}(x_2)$, which we denote by \bar{x} . Then, by lifting a loop based at \bar{x} which turns around z_0 for an appropriate number of times, we see that x'_1 is connected to x_2 in $\mathbb{Z}_{\mathbb{E}^2 \setminus \{z_0\}, \gamma}$. Therefore, $\mathbb{Z}_{\mathbb{E}^2 \setminus \{z_0\}, \gamma}$ is path-wise connected.

Moreover, the lift of a loop ℓ in $\mathbb{E}^2 \setminus \{z_0\}$ by $\pi_{z_0, \gamma}$ is a loop if and only if its winding number around z_0 vanishes. This is because the section $\sigma_{z_0, \gamma}$ over ℓ winds around S^1 by the same number of times as it winds around z_0 . This implies that the action of $\pi_1(\mathbb{E}^2 \setminus \{z_0\})$ on $\mathbb{Z}_{\mathbb{E}^2 \setminus \{z_0\}, \gamma}$ is effective. Therefore, $\pi_{z_0, \gamma}$ is a universal covering. This completes the proof. \square

Remark 2.3. It should be noted that $\mathbb{Z}_{\mathbb{E}^2 \setminus \{z_0\}, \gamma}$ is embedded in $\mathbb{E}_{\mathbb{E}^2 \setminus \{z_0\}} \subset \mathbb{E}^3$. This represents a screw dislocation in a crystal in continuum picture. The point z_0 corresponds to the position of the dislocation line.

Remark 2.4. A standard universal covering space $\mathbb{Z}_{\mathbb{E}^2 \setminus \{z_0\}}$ of $\mathbb{E}^2 \setminus \{z_0\}$ is constructed as follows. Fixing a point $x_0 \in \mathbb{E}^2 \setminus \{z_0\}$, we consider the path space (see [BT])

$$\text{Path}(\mathbb{E}^2 \setminus \{z_0\}) := \{\text{continuous maps } \mu : [0, 1] \rightarrow \mathbb{E}^2 \setminus \{z_0\} \mid \mu(0) = x_0\} / \sim,$$

where two paths μ and ν are equivalent, written as $\mu \sim \nu$, if $\mu(1) = \nu(1)$ and μ is homotopic to ν relative to end points in $\mathbb{E}^2 \setminus \{z_0\}$. The path space is the quotient space with respect to the equivalence, where it is endowed with the natural topology induced from that of the locally simply connected space $\mathbb{E}^2 \setminus \{z_0\}$. Then the map $\pi_{\text{Path}} : \text{Path}(\mathbb{E}^2 \setminus \{z_0\}) \ni \mu \mapsto \mu(1) \in \mathbb{E}^2 \setminus \{z_0\}$ defines a universal covering. Note that $\pi_{\text{Path}}^{-1}(z)$, $z \in \mathbb{E}^2 \setminus \{z_0\}$, is regarded as the set of winding numbers around z_0 , i.e. $\pi_{\text{Path}}^{-1}(z) = \mathbb{Z}$ up to a shift. Then, we define

$$\mathbb{Z}_{\mathbb{E}^2 \setminus \{z_0\}} := \text{Path}(\mathbb{E}^2 \setminus \{z_0\}).$$

It should be noted that the space obtained does not depend on the choice of the point x_0 , up to a covering equivalence.

By virtue of Lemma 2.2 together with the uniqueness of the universal covering, we can construct an embedding $\widehat{\varphi}_{z_0, \delta} : \mathbb{Z}_{\mathbb{E}^2 \setminus \{z_0\}} \rightarrow \mathbb{E}_{\mathbb{E}^2 \setminus \{z_0\}}$ such that the diagram

$$\begin{array}{ccc} \mathbb{Z}_{\mathbb{E}^2 \setminus \{z_0\}} & \xrightarrow{\widehat{\varphi}_{z_0, \delta}} & \mathbb{E}_{\mathbb{E}^2 \setminus \{z_0\}} \\ & \searrow \pi_{\text{Path}} & \swarrow \pi_{\mathbb{E}|\mathbb{E}_{\mathbb{E}^2 \setminus \{z_0\}}} \\ & \mathbb{E}^2 \setminus \{z_0\} & \end{array}$$

commutes and

$$\widehat{\varphi}_{z_0, \delta}(\mathbb{Z}_{\mathbb{E}^2 \setminus \{z_0\}}) = \mathbb{Z}_{\mathbb{E}^2 \setminus \{z_0\}, \gamma} \subset \mathbb{E}^3$$

holds for $\gamma = \exp(2\pi\sqrt{-1}\delta/d)$. In other words, we have the sequence

$$(2.4) \quad \mathbb{Z}_{\mathbb{E}^2 \setminus \{z_0\}} \xrightarrow{\widehat{\varphi}_{z_0, \delta}} \mathbb{E}_{\mathbb{E}^2 \setminus \{z_0\}} \xrightarrow{\widehat{\psi}} \mathcal{S}_{\mathbb{E}^2 \setminus \{z_0\}}^1$$

as a non-trivial analogue of (2.3) in such a way that $\widehat{\psi} \circ \widehat{\varphi}_{z_0, \delta}(\mathbb{Z}_{\mathbb{E}^2 \setminus \{z_0\}}) = \sigma_{z_0, \gamma}(\mathbb{E}^2 \setminus \{z_0\})$ and that $\widehat{\varphi}_{z_0, \delta}(\mathbb{Z}_{\mathbb{E}^2 \setminus \{z_0\}})$ represents a single screw dislocation in a crystal.

2.3. Multi-Screw Dislocation in Continuum Picture. Let us now consider multiple screw dislocations that are parallel to each other. They are described as follows.

Let $\mathcal{S} = \mathcal{S}_+ \amalg \mathcal{S}_-$ be a finite subset of \mathbb{E}^2 , which is divided into disjoint subsets \mathcal{S}_+ and \mathcal{S}_- . Let us consider the trivial bundles $\mathbb{E}_{\mathbb{E}^2 \setminus \mathcal{S}}$ and $\mathcal{S}_{\mathbb{E}^2 \setminus \mathcal{S}}^1$ over $\mathbb{E}^2 \setminus \mathcal{S}$ as in the previous subsections. Then, we consider the section $\sigma_{\mathcal{S}, \gamma} \in \Gamma(\mathbb{E}^2 \setminus \mathcal{S}, \mathcal{S}_{\mathbb{E}^2 \setminus \mathcal{S}}^1)$ defined by

$$(2.5) \quad \sigma_{\mathcal{S}, \gamma}(z) = \left(\gamma \prod_{z_i \in \mathcal{S}_+} \frac{z - z_i}{|z - z_i|} \cdot \prod_{z_j \in \mathcal{S}_-} \frac{\overline{z - z_j}}{|z - z_j|}, z \right) \text{ for } z \in \mathbb{E}^2 \setminus \mathcal{S} = \mathbb{C} \setminus \mathcal{S},$$

where $\overline{z - z_j}$ is the complex conjugate of $z - z_j$. We enumerate the points in \mathcal{S} in such a way that

$$\mathcal{S}_+ = \{z_1, z_2, \dots, z_s\}, \quad \mathcal{S}_- = \{z_{s+1}, z_{s+2}, \dots, z_{s+t}\},$$

where $n = s + t$ is the cardinality of \mathcal{S} .

Definition 2.5. Set

$$\mathbb{Z}_{\mathbb{E}^2 \setminus \mathcal{S}, \gamma} := \widehat{\psi}^{-1}(\sigma_{\mathcal{S}, \gamma}(\mathbb{E}^2 \setminus \mathcal{S})) \subset \mathbb{E}^3 \setminus \pi_{\mathbb{E}}^{-1}(\mathcal{S}) \subset \mathbb{E}^3$$

and define $\pi_{\mathcal{S}, \gamma} : \mathbb{Z}_{\mathbb{E}^2 \setminus \mathcal{S}, \gamma} \rightarrow \mathbb{E}^2 \setminus \mathcal{S}$ by $\pi_{\mathcal{S}, \gamma} = \pi_{\mathbb{E}}|_{\mathbb{Z}_{\mathbb{E}^2 \setminus \mathcal{S}, \gamma}}$.

As in Lemma 2.2, we see that $\pi_{\mathcal{S}, \gamma}$ defines a covering map. Note also that the covering space $\mathbb{Z}_{\mathbb{E}^2 \setminus \mathcal{S}, \gamma}$ of $\mathbb{E}^2 \setminus \mathcal{S}$ is realized in \mathbb{E}^3 . This represents multiple parallel screw dislocations in a crystal in continuum picture. The set \mathcal{S} corresponds to the positions of the dislocation lines.

Now, let us clarify the nature of the covering $\pi_{\mathcal{S},\gamma} : \mathbb{Z}_{\mathbb{E}^2 \setminus \mathcal{S},\gamma} \rightarrow \mathbb{E}^2 \setminus \mathcal{S}$. As in Remark 2.4, we can define the path space

$$\text{Path}(\mathbb{E}^2 \setminus \mathcal{S}) := \{\text{continuous maps } \mu : [0, 1] \rightarrow \mathbb{E}^2 \setminus \mathcal{S} \mid \mu(0) = x_0\} / \sim,$$

using the same equivalence relation, where we fix a point $x_0 \in \mathbb{E}^2 \setminus \mathcal{S}$. This is the universal covering space of $\mathbb{E}^2 \setminus \mathcal{S}$. However, for our purpose, this space is too big, and we need to take certain quotients.

Note that the fundamental group $G = \pi_1(\mathbb{E}^2 \setminus \mathcal{S}, x_0)$ is a free group of rank n generated by m_1, m_2, \dots, m_n , where m_i is the element of G represented by a loop based at x_0 which turns around z_i once in the counterclockwise direction and which does not turn around z_j , $j \neq i$. Let $G' = [G, G]$ be the commutator subgroup of G . By taking the orbit space under the natural action of G' , we get the universal abelian covering space of $\mathbb{E} \setminus \mathcal{S}$, denoted by $\text{Path}^a(\mathbb{E}^2 \setminus \mathcal{S})$. In other words, we have

$$\text{Path}^a(\mathbb{E}^2 \setminus \mathcal{S}) := \{\text{continuous maps } \mu : [0, 1] \rightarrow \mathbb{E}^2 \setminus \mathcal{S} \mid \mu(0) = x_0\} / \sim_a,$$

where for two paths μ and ν , we have $\mu \sim_a \nu$ if $\mu(1) = \nu(1)$ and the loop $\mu * \bar{\nu}$ based at x_0 represents an element of G' , where $\mu * \bar{\nu}$ denotes the product path of μ and the inverse path of ν .

Note that the homology group $H_1(\mathbb{E}^2 \setminus \mathcal{S}; \mathbb{Z})$ is isomorphic to \mathbb{Z}^n , which is freely generated by the homology classes $[m_1], [m_2], \dots, [m_n]$ represented by m_1, m_2, \dots, m_n , respectively. Note also that $H_1(\mathbb{E}^2 \setminus \mathcal{S}; \mathbb{Z})$ is isomorphic to the quotient group G/G' . An arbitrary element κ of $H_1(\mathbb{E}^2 \setminus \mathcal{S}; \mathbb{Z})$ is represented as $\sum_i w_i [m_i]$, where $w_i \in \mathbb{Z}$ is the winding number of κ around z_i in the direction of m_i . Therefore, for a loop ℓ in $\mathbb{E}^2 \setminus \mathcal{S}$, its lift in $\text{Path}^a(\mathbb{E}^2 \setminus \mathcal{S})$ is a loop if and only if the winding number of ℓ around each point of \mathcal{S} vanishes.

Let us now define

$$\mathbb{Z}_{\mathbb{E}^2 \setminus \mathcal{S}}^n := \text{Path}^a(\mathbb{E}^2 \setminus \mathcal{S}), \quad \pi_{\text{Path}^a} : \mathbb{Z}_{\mathbb{E}^2 \setminus \mathcal{S}}^n \rightarrow \mathbb{E}^2 \setminus \mathcal{S},$$

where π_{Path^a} sends the class of each path to its terminal point. Note that π_{Path^a} defines a covering, and that for each $z \in \mathbb{E}^2 \setminus \mathcal{S}$, $\pi_{\text{Path}^a}^{-1}(z)$ can be identified with \mathbb{Z}^n up to a certain ‘‘shift’’.

Let us now take further quotients. Let $h : \pi_1(\mathbb{E}^2 \setminus \mathcal{S}, x_0) \rightarrow \mathbb{Z}$ be the homomorphism defined by

$$h(m_i) = \begin{cases} 1, & 1 \leq i \leq s, \\ -1, & s+1 \leq i \leq s+t. \end{cases}$$

Since \mathbb{Z} is abelian, the kernel H of h contains G' . Let $\mathbb{Z}_{\mathbb{E}^2 \setminus \mathcal{S}}$ be the orbit space of $\text{Path}(\mathbb{E}^2 \setminus \mathcal{S})$ under the natural action of H . In other words, we have

$$\mathbb{Z}_{\mathbb{E}^2 \setminus \mathcal{S}} := \{\text{continuous maps } \mu : [0, 1] \rightarrow \mathbb{E}^2 \setminus \mathcal{S} \mid \mu(0) = x_0\} / \sim_h,$$

where for two paths μ and ν , we have $\mu \sim_h \nu$ if $\mu(1) = \nu(1)$ and the loop $\mu * \bar{\nu}$ based at x_0 represents an element of H . We have a natural projection $\pi_H : \mathbb{Z}_{\mathbb{E}^2 \setminus \mathcal{S}} \rightarrow \mathbb{E}^2 \setminus \mathcal{S}$ which sends the class of each path to its terminal point. Note that π_H defines a covering map.

Proposition 2.6. *The coverings $\pi_{\mathcal{S},\gamma} : \mathbb{Z}_{\mathbb{E}^2 \setminus \mathcal{S},\gamma} \rightarrow \mathbb{E}^2 \setminus \mathcal{S}$ and $\pi_H : \mathbb{Z}_{\mathbb{E}^2 \setminus \mathcal{S}} \rightarrow \mathbb{E}^2 \setminus \mathcal{S}$ are equivalent.*

Proof. Fix a point $\tilde{x}_0 \in \mathbb{Z}_{\mathbb{E}^2 \setminus \mathcal{S},\gamma}$ such that $\pi_{\mathcal{S},\gamma}(\tilde{x}_0) = x_0$. We define the map $\Phi : \mathbb{Z}_{\mathbb{E}^2 \setminus \mathcal{S},\gamma} \rightarrow \mathbb{Z}_{\mathbb{E}^2 \setminus \mathcal{S}}$ as follows. For $x \in \mathbb{Z}_{\mathbb{E}^2 \setminus \mathcal{S},\gamma}$, since $\mathbb{Z}_{\mathbb{E}^2 \setminus \mathcal{S},\gamma}$ is connected, we can find a path $\tilde{\mu}$ connecting \tilde{x}_0 and x . Then, the composition $\mu = \pi_{\mathcal{S},\gamma} \circ \tilde{\mu}$ can be regarded as an element of $\mathbb{Z}_{\mathbb{E}^2 \setminus \mathcal{S}}$ as a continuous path. We see that this map Φ is well-defined and injective, by observing that the lift of a loop λ based at x_0 in $\mathbb{E}^2 \setminus \mathcal{S}$ with respect to $\pi_{\mathcal{S},\gamma}$ is again a loop if and only if $h([\lambda])$ vanishes, where $[\lambda] \in \pi_1(\mathbb{E}^2 \setminus \mathcal{S}, x_0)$ is the class represented by λ . Furthermore, by the existence of a lift for paths, we see that Φ is surjective. Since, we see easily that Φ is a local homeomorphism, we conclude that the map Φ gives the desired equivalence of coverings. \square

As a consequence, we can construct an embedding $\hat{\varphi}_{\mathcal{S},\delta} : \mathbb{Z}_{\mathbb{E}^2 \setminus \mathcal{S}} \rightarrow \mathbb{E}_{\mathbb{E}^2 \setminus \mathcal{S}}$ such that the diagram

$$\begin{array}{ccc} \mathbb{Z}_{\mathbb{E}^2 \setminus \mathcal{S}} & \xrightarrow{\hat{\varphi}_{\mathcal{S},\delta}} & \mathbb{E}_{\mathbb{E}^2 \setminus \mathcal{S}} \\ & \searrow \pi_H & \swarrow \pi_{\mathbb{E}|\mathbb{E}_{\mathbb{E}^2 \setminus \mathcal{S}}} \\ & \mathbb{E}^2 \setminus \mathcal{S} & \end{array}$$

commutes and

$$\hat{\varphi}_{\mathcal{S},\delta}(\mathbb{Z}_{\mathbb{E}^2 \setminus \mathcal{S}}) = \mathbb{Z}_{\mathbb{E}^2 \setminus \mathcal{S},\gamma} \subset \mathbb{E}^3$$

holds for $\gamma = \exp(2\pi\sqrt{-1}\delta/d)$. In other words, we have the sequence

$$(2.6) \quad \mathbb{Z}_{\mathbb{E}^2 \setminus \mathcal{S}} \xrightarrow{\hat{\varphi}_{\mathcal{S},\delta}} \mathbb{E}_{\mathbb{E}^2 \setminus \mathcal{S}} \xrightarrow{\hat{\psi}} \mathcal{S}_{\mathbb{E}^2 \setminus \mathcal{S}}^1$$

as a non-trivial analogue of (2.3) such that $\hat{\psi} \circ \hat{\varphi}_{\mathcal{S},\delta}(\mathbb{Z}_{\mathbb{E}^2 \setminus \mathcal{S}}) = \sigma_{\mathcal{S},\gamma}(\mathbb{E}^2 \setminus \mathcal{S})$ and that $\hat{\varphi}_{\mathcal{S},\delta}(\mathbb{Z}_{\mathbb{E}^2 \setminus \mathcal{S}})$ represents a multiple parallel screw dislocations in a crystal, which generalizes (2.4).

In the following sections, we will consider discrete pictures of dislocations, which will be embedded in these continuum pictures.

3. ABELIAN GROUP STRUCTURE OF SC LATTICE AND ITS SCREW DISLOCATIONS

3.1. Algebraic Structure of SC lattice. The simple cubic (SC) lattice is usually expressed by the additive free abelian group

$$\mathbb{A}_3^a := \mathbb{Z}a_1 + \mathbb{Z}a_2 + \mathbb{Z}a_3 = \langle a_1, a_2, a_3 \rangle_{\mathbb{Z}},$$

which is generated by three elements a_1, a_2 and a_3 . Here, by identifying a_1 with $(a, 0, 0)$, a_2 with $(0, a, 0)$, and a_3 with $(0, 0, a)$ in \mathbb{R}^3 endowed with the euclidean inner product, we see that \mathbb{A}_3^a is naturally embedded in \mathbb{R}^3 as a SC lattice as shown in Figure 1 (a). We denote

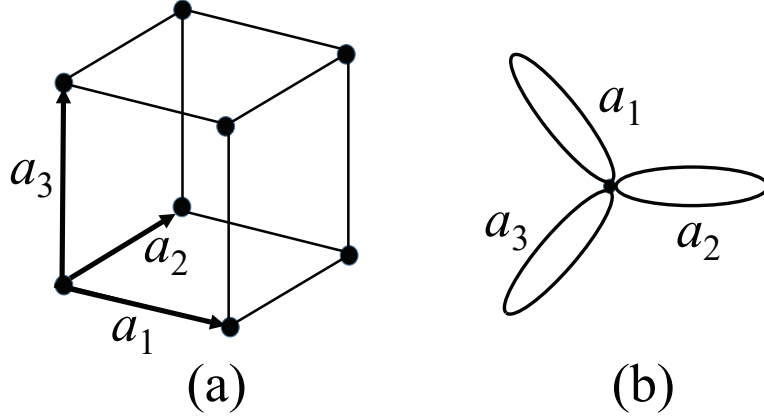


FIGURE 1. Simple cubic (SC) lattice

this embedding by $\iota_{\mathbb{A}_3} : \mathbb{A}_3^a \hookrightarrow \mathbb{R}^3$. Furthermore, we embed \mathbb{A}_3^a into the euclidean 3-space \mathbb{E}^3 as follows. By fixing $\delta = (\delta_1, \delta_2, \delta_3) \in \mathbb{E}^3$ and $g \in \text{SO}(3)$, we define $\iota_{\mathbb{A}_3, \delta, g} : \mathbb{A}_3^a \hookrightarrow \mathbb{E}^3$ by

$$\iota_{\mathbb{A}_3, \delta, g}(n_1 a_1 + n_2 a_2 + n_3 a_3) = g(n_1 a, n_2 a, n_3 a) + (\delta_1, \delta_2, \delta_3)$$

for $n_1, n_2, n_3 \in \mathbb{Z}$. When $g \in \text{SO}(3)$ is the identity, we denote it by $\iota_{\mathbb{A}_3, \delta} : \mathbb{A}_3^a \hookrightarrow \mathbb{E}^3$, which is defined by

$$(3.1) \quad \iota_{\mathbb{A}_3, \delta}(n_1 a_1 + n_2 a_2 + n_3 a_3) = (n_1 a, n_2 a, n_3 a) + (\delta_1, \delta_2, \delta_3).$$

Remark 3.1. We have the natural action of the discrete subgroup of $\text{SO}(3)$ on the SC lattice [CS, I, Koh, S], which is isomorphic to the symmetric group S_4 on a set of four elements [I], although it does not play an important role in this article.

In this article, we often use the multiplicative abelian group

$$\mathbb{A}_3 := \{\alpha_1^{n_1} \alpha_2^{n_2} \alpha_3^{n_3} \mid \text{abelian}, n_1, n_2, n_3 \in \mathbb{Z}\}$$

rather than the additive group \mathbb{A}_3^a for convenience. Here, α_b corresponds to a_b , $b = 1, 2, 3$. Through the natural identification of \mathbb{A}_3 with \mathbb{A}_3^a , we continue to use the symbols $\iota_{\mathbb{A}_3}$ and $\iota_{\mathbb{A}_3, \delta}$ also for \mathbb{A}_3 by abuse of notation.

Remark 3.2. The SC lattice is regarded as the universal abelian covering of a certain geometric object. In fact, the SC lattice is expressed by the graph as depicted in Figure 1 (b) [S]. More precisely, the universal abelian covering of the graph given by Figure 1 (b) coincides with the Cayley graph of the group \mathbb{A}_3 with respect to the generating set $\{\alpha_1, \alpha_2, \alpha_3\}$.



FIGURE 2. Fibering structure of simple cubic lattice

3.2. Fibering Structure of SC Lattice: $(0, 0, 1)$ -direction. Let us introduce the group ring

$$\mathbb{C}[\mathbb{A}_3] = \mathbb{C}[\alpha_1, \alpha_2, \alpha_3, \alpha_1^{-1}, \alpha_2^{-1}, \alpha_3^{-1}]$$

in order to consider the fibering structure of \mathbb{A}_3 (and that of \mathbb{A}_3^a). Its projection to the 2-dimensional space corresponds to taking the quotient as

$$\mathbb{C}[\mathbb{A}_3]/(\alpha_3 - 1) = \mathbb{C}[\alpha_1, \alpha_2, \alpha_1^{-1}, \alpha_2^{-1}] =: \mathbb{C}[\mathbb{A}_2],$$

where

$$\mathbb{A}_2 := \{\alpha_1^{n_1} \alpha_2^{n_2} \mid \text{abelian}, n_1, n_2 \in \mathbb{Z}\},$$

which is group-isomorphic to $\mathbb{A}_2^a := \mathbb{Z}a_1 + \mathbb{Z}a_2$, and $(\alpha_3 - 1)$ is the ideal generated by $\alpha_3 - 1$. As in the case of \mathbb{A}_3 , by assuming that α_1 and α_2 correspond to $(a, 0)$ and $(0, a)$ in \mathbb{R}^2 , respectively, we may regard $\mathbb{A}_2^a \approx \mathbb{A}_2$ as being also naturally embedded in \mathbb{R}^2 . Thus, we have natural embeddings $\iota_{\mathbb{A}_2} : \mathbb{A}_2 \hookrightarrow \mathbb{R}^2$ and $\iota_{\mathbb{A}_2, \bar{\delta}} : \mathbb{A}_2 \hookrightarrow \mathbb{E}^2$ for $\bar{\delta} = (\delta_1, \delta_2) \in \mathbb{E}^2$.

The projection above “induces” the fibering structure

$$\begin{array}{ccc} \mathbb{Z} & \longrightarrow & \mathbb{A}_3 \\ & & \downarrow \varpi \\ & & \mathbb{A}_2, \end{array}$$

where ϖ is the projection defined by $\varpi(\alpha_1^{n_1} \alpha_2^{n_2} \alpha_3^{n_3}) = \alpha_1^{n_1} \alpha_2^{n_2}$, $n_1, n_2, n_3 \in \mathbb{Z}$. Its graph expression is given by Figure 2: more precisely, the Cayley graph of \mathbb{A}_2 with respect to the generating set $\{\alpha_1, \alpha_2, \alpha_3\}$ coincides with the graph depicted in Figure 2. We will see that the above fibering structure is essential in our description of screw dislocations.

Note that we may regard the group ring $\mathbb{C}[\mathbb{A}_2]$ as a set of certain complex valued functions on \mathbb{A}_2 : for an element of $f \in \mathbb{C}[\mathbb{A}_2]$, we have the complex number $f(n_1, n_2) \in \mathbb{C}$

for every element $\alpha_1^{n_1}\alpha_2^{n_2} \in \mathbb{A}_2$ in such a way that we have

$$f = \sum_{(n_1, n_2) \in \mathbb{Z}^2} f(n_1, n_2) \alpha_1^{n_1} \alpha_2^{n_2}.$$

In this case, f can take non-zero complex values only on a finite number of elements of \mathbb{A}_2 . We extend this space to the whole function space $\mathcal{F}(\mathcal{A}_p, \mathbb{C})$, where we use the symbol \mathcal{A}_p for \mathbb{A}_2 viewed as a set or as a discrete topological space, i.e.,

$$\mathcal{A}_p := \{(n_1 a, n_2 a) \mid n_1, n_2 \in \mathbb{Z}\}.$$

We denote by $S_{\mathcal{A}_p}^1$ the trivial S^1 -bundle over \mathcal{A}_p . For every fiber bundle $F_{\mathbb{E}^2}$ over \mathbb{E}^2 and for $\bar{\delta} = (\delta_1, \delta_2) \in \mathbb{E}^2$, by the natural embedding $i_{\bar{\delta}}^{\text{SC}} : \mathcal{A}_p \hookrightarrow \mathbb{E}^2$ defined by $(n_1 a, n_2 a) \mapsto (n_1 a + \delta_1, n_2 a + \delta_2)$, we have the pullback bundle $F_{\mathcal{A}_p}$ over \mathcal{A}_p .

Let $\mathcal{S} = \mathcal{S}_+ \amalg \mathcal{S}_-$ be a finite subset in \mathbb{E}^2 as in Subsection 2.3. In the following, we assume that $\bar{\delta} \in \mathbb{E}^2$ satisfies $i_{\bar{\delta}}^{\text{SC}}(\mathcal{A}_p) \cap \mathcal{S} = \emptyset$. Then, the map $i_{\bar{\delta}}^{\text{SC}}$ is regarded as the embedding $i_{\bar{\delta}}^{\text{SC}} : \mathcal{A}_p \hookrightarrow \mathbb{E}^2 \setminus \mathcal{S}$. Thus, we have the following.

Lemma 3.3. *For every fiber bundle $F_{\mathbb{E}^2 \setminus \mathcal{S}}$ over $\mathbb{E}^2 \setminus \mathcal{S}$, by the embedding $i_{\bar{\delta}}^{\text{SC}} : \mathcal{A}_p \hookrightarrow \mathbb{E}^2 \setminus \mathcal{S}$, we have the pullback bundle $F_{\mathcal{A}_p}$ that satisfies the commutative diagram*

$$\begin{array}{ccc} F_{\mathcal{A}_p} & \xrightarrow{i_{\bar{\delta}}^{\text{SC}}} & F_{\mathbb{E}^2 \setminus \mathcal{S}} \\ \downarrow & & \downarrow \\ \mathcal{A}_p & \xrightarrow{i_{\bar{\delta}}^{\text{SC}}} & \mathbb{E}^2 \setminus \mathcal{S}, \end{array}$$

where the vertical maps are the projections of the fiber bundles and $i_{\bar{\delta}}^{\text{SC}}$ is the bundle map induced by $i_{\bar{\delta}}^{\text{SC}}$.

Recall that in Section 2, we have fixed $d > 0$. In the following, we set $d = a$. Using the above pullback diagram (Cartesian square), we have the following.

Lemma 3.4. *We have the following commutative diagram:*

$$\begin{array}{ccc} \mathbb{E}_{\mathcal{A}_p} & \xrightarrow{i_{\bar{\delta}}^{\text{SC}}} & \mathbb{E}_{\mathbb{E}^2 \setminus \mathcal{S}} \\ \downarrow & & \downarrow \\ \mathcal{A}_p & \xrightarrow{i_{\bar{\delta}}^{\text{SC}}} & \mathbb{E}^2 \setminus \mathcal{S} \\ \uparrow & & \uparrow \\ S_{\mathcal{A}_p}^1 & \xrightarrow{i_{\bar{\delta}}^{\text{SC}}} & S_{\mathbb{E}^2 \setminus \mathcal{S}}^1 \end{array} \quad \widehat{\psi}$$

where the straight vertical arrows are projections of the fiber bundles and $\widehat{\psi}$ are the bundle maps induced by ψ defined in Section 2.

The above lemma is easy to prove, and hence we omit the proof.

The following proposition corresponds to the case where $\mathcal{S} = \emptyset$ and the proof is left to the reader.

Proposition 3.5. *Set $\gamma = \exp(2\pi\sqrt{-1}\delta_3/a) \in S^1$ for a $\delta_3 \in \mathbb{R}$ and consider the global section $\check{\sigma}_\gamma \in \Gamma(\mathcal{A}_p, S^1_{\mathcal{A}_p})$ that constantly takes the value γ . Then, we have that*

$$\hat{\iota}_\delta^{\text{SC}} \left(\widehat{\psi}^{-1}(\check{\sigma}_\gamma(\mathcal{A}_p)) \right) = \hat{\iota}_\delta^{\text{SC}} \left(\frac{a}{2\pi\sqrt{-1}} \exp^{-1}(\check{\sigma}_\gamma(\mathcal{A}_p)) \right) \subset \mathbb{E}_{\mathbb{E}^2 \setminus \mathcal{S}} \subset \mathbb{E}^3$$

coincides with $\iota_{\mathbb{A}_3, \delta}(\mathbb{A}_3^a)$ as a subset in \mathbb{E}^3 for $\delta = (\bar{\delta}, \delta_3) = (\delta_1, \delta_2, \delta_3)$, i.e.,

$$\iota_{\mathbb{A}_3, \delta}(\mathbb{A}_3^a) = \hat{\iota}_\delta^{\text{SC}} \left(\widehat{\psi}^{-1}(\check{\sigma}_\gamma(\mathcal{A}_p)) \right).$$

In other words, the SC lattice without dislocation can be interpreted as the inverse image by $\widehat{\psi}$ of a constant section $\check{\sigma}_\gamma$ of the trivial S^1 -bundle.

3.3. Screw Dislocation in Simple Cubic Lattice. A screw dislocation in the simple cubic lattice appears along the $(0, 0, 1)$ -direction [N]. In other words, the Burgers vector is parallel to the $(0, 0, 1)$ -direction.

Using the fibering structure of Lemma 3.4, for the case where $\mathcal{S} = \{z_0\}$, $z_0 \in \mathbb{C}$, we can describe a single screw dislocation in the SC lattice as follows, whose proof is straightforward. Our principal idea is to use a section in $\Gamma(\mathcal{A}_p, S^1_{\mathcal{A}_p})$ in order to describe a screw dislocation.

Proposition 3.6. *Let us define the section $\check{\sigma}_{z_0, \gamma} \in \Gamma(\mathcal{A}_p, S^1_{\mathcal{A}_p})$ by*

$$\check{\sigma}_{z_0, \gamma}(\ell_1 a, \ell_2 a) = \left(\gamma \frac{(\ell_1 a + \ell_2 a \sqrt{-1}) - z_0}{|(\ell_1 a + \ell_2 a \sqrt{-1}) - z_0|}, (\ell_1 a, \ell_2 a) \right), \quad (\ell_1 a, \ell_2 a) \in \mathcal{A}_p,$$

where $\gamma = \exp(2\pi\sqrt{-1}\delta_3/a) \in S^1$. Then, the screw dislocation around z_0 given by

$$\mathcal{D}_{z_0}^{\text{SC}} := \hat{\iota}_\delta^{\text{SC}} \left(\widehat{\psi}^{-1}(\check{\sigma}_{z_0, \gamma}(\mathcal{A}_p)) \right) = \hat{\iota}_\delta^{\text{SC}} \left(\frac{a}{2\pi\sqrt{-1}} \exp^{-1}(\check{\sigma}_{z_0, \gamma}(\mathcal{A}_p)) \right)$$

is realized in \mathbb{E}^3 .

We note that $\mathcal{D}_{z_0}^{\text{SC}}$ can be regarded as a kind of a ‘‘covering space of the lattice \mathcal{A}_p ’’.

Remark 3.7. (1) Let $\mathbb{Z}_{\mathcal{A}_p, \gamma}$ be the pullback of $\mathbb{Z}_{\mathbb{E}^2 \setminus \{z_0\}, \gamma}$ by $\iota_\delta^{\text{SC}} : \mathcal{A}_p \rightarrow \mathbb{E}^2 \setminus \{z_0\}$, and $\hat{\iota}_\delta^{\text{SC}} : \mathbb{Z}_{\mathcal{A}_p, \gamma} \rightarrow \mathbb{Z}_{\mathbb{E}^2 \setminus \{z_0\}, \gamma}$ the induced bundle map. Then, we have the equality

$$\mathcal{D}_{z_0}^{\text{SC}} = \hat{\iota}_\delta^{\text{SC}}(\mathbb{Z}_{\mathcal{A}_p, \gamma}),$$

which follows directly from the definition of $\mathbb{Z}_{\mathbb{E}^2 \setminus \{z_0\}, \gamma}$ given in Subsection 2.2.

(2) Here, $\mathcal{S} = \{z_0\}$ corresponds to the position of the dislocation line (see Figure 3). As has been mentioned in the continuum model, $\mathcal{D}_{z_0}^{\text{SC}}$ naturally embeds into the path space $\mathbb{Z}_{\mathbb{E}^2 \setminus \{z_0\}}$ via the identification $\widehat{\varphi}_{z_0, \delta_3} : \mathbb{Z}_{\mathbb{E}^2 \setminus \{z_0\}} \rightarrow \mathbb{Z}_{\mathbb{E}^2 \setminus \{z_0\}, \gamma}$.

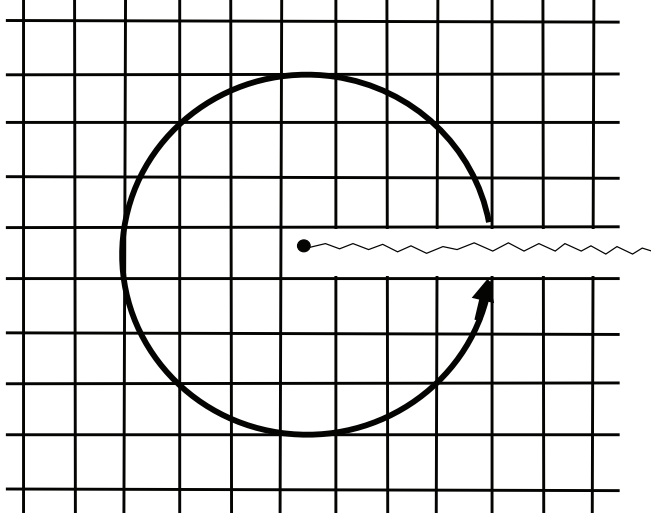


FIGURE 3. Screw dislocation in the SC lattice: the lattice points correspond to $\mathcal{A}_p \subset \mathbb{E}^2$ and the center point is z_0 .

A parallel multi-screw dislocation is described as follows. Let us define the section $\check{\sigma}_{\mathcal{S},\gamma} \in \Gamma(\mathcal{A}_p, S_{\mathcal{A}_p}^1)$ by

$$\check{\sigma}_{\mathcal{S},\gamma}(l_1a, l_2a) = \left(\gamma \prod_{z_i \in \mathcal{S}_+} \frac{(l_1a + l_2a\sqrt{-1}) - z_i}{|(l_1a + l_2a\sqrt{-1}) - z_i|} \prod_{z_j \in \mathcal{S}_-} \frac{\overline{(l_1a + l_2a\sqrt{-1}) - z_j}}{|(l_1a + l_2a\sqrt{-1}) - z_j|}, (l_1a, l_2a) \right),$$

$(l_1a, l_2a) \in \mathcal{A}_p.$

Then, we have the following, whose proof is straightforward.

Proposition 3.8. *The parallel multi-screw dislocation $\mathcal{D}_{\mathcal{S}}^{\text{SC}}$ given by*

$$\mathcal{D}_{\mathcal{S}}^{\text{SC}} = \hat{\iota}_{\delta}^{\text{SC}} \left(\widehat{\psi}^{-1}(\check{\sigma}_{\mathcal{S},\gamma}(\mathcal{A}_p)) \right) = \hat{\iota}_{\delta}^{\text{SC}} \left(\frac{a}{2\pi\sqrt{-1}} \exp^{-1}(\check{\sigma}_{\mathcal{S},\gamma}(\mathcal{A}_p)) \right)$$

is realized in \mathbb{E}^3 as a subset of $\mathbb{Z}_{\mathbb{E}^2 \setminus \mathcal{S},\gamma}$, where \mathcal{S} corresponds to the position of the dislocation lines.

4. FIBERING STRUCTURE OF BCC LATTICE: (1, 1, 1)-DIRECTION AND ITS SCREW DISLOCATION

4.1. Fiberling Structure of SC Lattice: (1, 1, 1)-direction. In this subsection, let us first consider the fiberling structure along the (1, 1, 1)-direction of the simple cubic

lattice. Although a screw dislocation does not occur along this direction physically, this construction is useful for analyzing the case of the BCC lattice.

This structure is a little bit complicated; however, our algebraic approach makes the computation easy and enables us to have its discrete geometric interpretation. Let us consider the projection which corresponds to the quotient ring

$$\mathcal{R}_d = \mathbb{C}[\mathbb{A}_3]/(\alpha_1\alpha_2\alpha_3 - 1),$$

where \mathbb{A}_3 is the multiplicative free abelian group of rank 3 generated by α_1 , α_2 and α_3 .

For the vector $a_1 + a_2 + a_3 \in \mathbb{A}_3^a \subset \mathbb{R}^3$, we have the vanishing euclidean inner products

$$(a_1 - a_3, a_1 + a_2 + a_3) = 0, \quad (a_2 - a_3, a_1 + a_2 + a_3) = 0.$$

Therefore, $a_1 - a_3$ and $a_2 - a_3$ constitute a basis for the orthogonal complement of the vector $a_1 + a_2 + a_3$ in \mathbb{R}^3 . This space corresponds to the group ring generated by $\alpha_1\alpha_3^{-1}$ and $\alpha_2\alpha_3^{-1}$. In other words, we consider

$$\mathbb{A}_d := \{(\alpha_1\alpha_3^{-1})^{\ell_1}(\alpha_2\alpha_3^{-1})^{\ell_2} \mid \ell_1, \ell_2 \in \mathbb{Z}\},$$

which is a subgroup of \mathbb{A}_3 . We also consider the group ring

$$\mathbb{C}[\mathbb{A}_d] = \mathbb{C}[\alpha_1\alpha_3^{-1}, \alpha_2\alpha_3^{-1}, \alpha_1^{-1}\alpha_3, \alpha_2^{-1}\alpha_3],$$

which is identified, under the relation $\alpha_1\alpha_2\alpha_3 = 1$, with

$$\mathbb{C}[\alpha_1\alpha_2^2, \alpha_1^2\alpha_2, \alpha_1^{-1}\alpha_2^{-2}, \alpha_1^{-2}\alpha_2^{-1}].$$

Note that, as $\mathbb{C}[\mathbb{A}_d]$ is a sub-ring of $\mathbb{C}[\mathbb{A}_3]$, \mathcal{R}_d is also considered to be a $\mathbb{C}[\mathbb{A}_d]$ -module.

Lemma 4.1. *We have a natural isomorphism as $\mathbb{C}[\mathbb{A}_d]$ -modules:*

$$\mathcal{R}_d \cong \mathbb{C}[\mathbb{A}_d] \oplus \mathbb{C}[\mathbb{A}_d]\alpha_1 \oplus \mathbb{C}[\mathbb{A}_d]\alpha_1\alpha_2.$$

Proof. First, note that every monomial of $\mathbb{C}[\mathbb{A}_3]$ has its own degree with respect to α_1, α_2 and α_3 , each of which has degree 1. Furthermore, it is easy to verify that a monomial has degree zero if and only if it belongs to $\mathbb{C}[\mathbb{A}_d]$. As a result, a monomial has degree r if and only if it belongs to $\mathbb{C}[\mathbb{A}_d]\alpha_1^r$, where we can replace α_1^r by any other monomial of degree r . Note that each $\mathbb{C}[\mathbb{A}_d]\alpha_1^r$ is a $\mathbb{C}[\mathbb{A}_d]$ -submodule of $\mathbb{C}[\mathbb{A}_3]$. Thus, we have the isomorphism

$$\mathbb{C}[\mathbb{A}_3] \cong \bigoplus_r \mathbb{C}[\mathbb{A}_d]\alpha_1^r$$

as $\mathbb{C}[\mathbb{A}_d]$ -modules.

Now, let us consider the $\mathbb{C}[\mathbb{A}_d]$ -module homomorphism induced by the inclusion

$$q : \bigoplus_{r=0}^2 \mathbb{C}[\mathbb{A}_d]\alpha_1^r \rightarrow \left(\bigoplus_r \mathbb{C}[\mathbb{A}_d]\alpha_1^r \right) / (1 - \alpha_1\alpha_2\alpha_3) \cong \mathbb{C}[\mathbb{A}_3]/(1 - \alpha_1\alpha_2\alpha_3),$$

where the ideal $(1 - \alpha_1\alpha_2\alpha_3)$ in the ring $\mathbb{C}[\mathbb{A}_3]$ is now considered as a $\mathbb{C}[\mathbb{A}_d]$ -submodule. We can easily show that this homomorphism q is injective, since every non-zero element of the submodule $(1 - \alpha_1\alpha_2\alpha_3)$ contains two non-zero monomials whose degrees are different by a non-zero multiple of 3. Furthermore, q is surjective, since we have $\mathbb{C}[\mathbb{A}_d]\alpha_1^r = \mathbb{C}[\mathbb{A}_d]\alpha_1^{r'}$ as

long as $r \equiv r' \pmod{3}$, under the relation $\alpha_1\alpha_2\alpha_3 = 1$. Furthermore, we have $\mathbb{C}[\mathbb{A}_d]\alpha_1^2 = \mathbb{C}[\mathbb{A}_d]\alpha_1\alpha_2$. Thus, we have the desired isomorphism of $\mathbb{C}[\mathbb{A}_d]$ -modules. This completes the proof. \square

Remark 4.2. Lemma 4.1 can be geometrically interpreted by using a cube as follows. Let us consider the cube whose vertices consist of $0, a_1, a_2, a_3, a_1 + a_2, a_2 + a_3, a_3 + a_1$ and $a_1 + a_2 + a_3$, which are identified with their corresponding elements $1, \alpha_1, \alpha_2, \alpha_3, \alpha_1\alpha_2, \alpha_2\alpha_3, \alpha_3\alpha_1$ and $\alpha_1\alpha_2\alpha_3$, respectively. We have the natural action of the symmetric group on the three elements α_1, α_2 and α_3 over the cube, which can be regarded as a subgroup of the octahedral group. The orbits of this action are given by $\{1\}, \{\alpha_1, \alpha_2, \alpha_3\}, \{\alpha_1\alpha_2, \alpha_2\alpha_3, \alpha_3\alpha_1\}$ and $\{\alpha_1\alpha_2\alpha_3\}$, which coincide with the classification by their degrees. By identifying 1 and $\alpha_1\alpha_2\alpha_3$, we get the three classes as described in Lemma 4.1.

Remark 4.3. We have another algebraic proof for Lemma 4.1 as follows.¹ Let us consider the diagonal monomorphism $\iota_3^{\text{diag}} : \mathbb{Z} \hookrightarrow \mathbb{A}_3^a$ defined by $\iota_3^{\text{diag}}(n) = n(a_1 + a_2 + a_3) \in \mathbb{A}_3^a$ for $n \in \mathbb{Z}$, and denote its image by $\mathbb{A}_3^{\text{diag}}$. Then we naturally have $\mathcal{R}_d \cong \mathbb{C}[\mathbb{A}_3^a/\mathbb{A}_3^{\text{diag}}]$. Furthermore, we also have the epimorphism $p_3 : \mathbb{A}_3^a \rightarrow \mathbb{Z}$ defined by $p_3(n_1a_1 + n_2a_2 + n_3a_3) = n_1 + n_2 + n_3$ for $n_1, n_2, n_3 \in \mathbb{Z}$. Setting $\mathbb{A}_d^a = \mathbb{Z}(a_1 - a_3) + \mathbb{Z}(a_2 - a_3) = \text{Ker } p_3$, we have the commutative diagram of exact rows

$$\begin{array}{ccccccc} 0 & \longrightarrow & \mathbb{Z} & \longrightarrow & 3\mathbb{Z} & \longrightarrow & 0 \\ & & \downarrow & & \downarrow & & \\ 0 & \longrightarrow & \mathbb{A}_d^a & \longrightarrow & \mathbb{A}_3^a & \xrightarrow{p_3} & \mathbb{Z} \longrightarrow 0, \end{array}$$

where the rightmost vertical map is the natural inclusion. By applying the snake lemma [L] to this diagram, we obtain the short exact sequence

$$0 \longrightarrow \mathbb{A}_d^a \longrightarrow \mathbb{A}_3^a/\mathbb{A}_3^{\text{diag}} \xrightarrow{\overline{p_3}} \mathbb{Z}/3\mathbb{Z} \longrightarrow 0,$$

where $\overline{p_3}$ is the epimorphism induced by p_3 . The inverse images of the three elements of $\mathbb{Z}/3\mathbb{Z}$ by $\overline{p_3}$ give the decomposition of $\mathbb{A}_3^a/\mathbb{A}_3^{\text{diag}}$ into three disjoint subsets, $\mathbb{A}_d^a, a_1 + \mathbb{A}_d^a$ and $a_1 + a_2 + \mathbb{A}_d^a$. This implies Lemma 4.1.

Remark 4.4. Lemma 4.1 means geometrically that the projection generates three sheets if we consider them embedded in \mathbb{E}^3 as shown in Figure 4. Each sheet can be regarded as a set given by the abelian group $\langle \alpha_1\alpha_3^{-1}, \alpha_2\alpha_3^{-1} \rangle$. More precisely, let us denote \mathbb{A}_3^a by \mathcal{A}_d when considered as a set. Then, we have the decomposition

$$\mathcal{A}_d := \mathcal{A}_d^{(0)} \amalg \mathcal{A}_d^{(1)} \amalg \mathcal{A}_d^{(2)},$$

¹The authors are indebted to an anonymous referee for this simple proof as well as that described in Remark 4.6 for Lemma 4.5.

where

$$\begin{aligned}\mathcal{A}_d^{(0)} &:= \{\ell_1(a_1 - a_3) + \ell_2(a_2 - a_3) \mid \ell_1, \ell_2 \in \mathbb{Z}\}, \\ \mathcal{A}_d^{(1)} &:= \{\ell_1(a_1 - a_3) + \ell_2(a_2 - a_3) + a_1 \mid \ell_1, \ell_2 \in \mathbb{Z}\}, \\ \mathcal{A}_d^{(2)} &:= \{\ell_1(a_1 - a_3) + \ell_2(a_2 - a_3) + a_1 + a_2 \mid \ell_1, \ell_2 \in \mathbb{Z}\}.\end{aligned}$$

Note that this corresponds exactly to the decomposition mentioned in Remark 4.3. This picture comes from the discrete nature of the lattice. The interval between the sheets is given by $\sqrt{3}a/3$.

4.2. Algebraic Structure of BCC Lattice. The BCC (body centered cubic) lattice is the lattice in \mathbb{R}^3 generated by a_1, a_2, a_3 and $(a_1 + a_2 + a_3)/2$. Algebraically, it is described as additive group (or \mathbb{Z} -module) by

$$\mathbb{B}^a := \langle a_1, a_2, a_3, b \rangle_{\mathbb{Z}} / \langle 2b - a_1 - a_2 - a_3 \rangle_{\mathbb{Z}},$$

where $\langle 2b - a_1 - a_2 - a_3 \rangle_{\mathbb{Z}}$ is the subgroup generated by $2b - a_1 - a_2 - a_3$ (see [CS, p. 116], for example). As in the case of the SC lattice, we assume that $a_1 = (a, 0, 0)$, $a_2 = (0, a, 0)$, $a_3 = (0, 0, a)$ in the euclidean 3-space \mathbb{E}^3 for a positive real number a as shown in Figure 5 (a). The generator b corresponds to the center point of the cube generated by a_1, a_2 and a_3 .

The lattice \mathbb{B}^a is group-isomorphic to the multiplicative group

$$\mathbb{B} := \{\alpha_1^{\ell_1} \alpha_2^{\ell_2} \alpha_3^{\ell_3} \beta^{\ell_4} \mid \text{abelian}, \ell_1, \ell_2, \ell_3, \ell_4 \in \mathbb{Z}, \beta^2 \alpha_1^{-1} \alpha_2^{-1} \alpha_3^{-1} = 1\}.$$

Let us denote by \mathbb{A}_4 the multiplicative free abelian group of rank 4 generated by $\alpha_1, \alpha_2, \alpha_3$ and β , i.e.,

$$\mathbb{A}_4 := \{\alpha_1^{\ell_1} \alpha_2^{\ell_2} \alpha_3^{\ell_3} \beta^{\ell_4} \mid \text{abelian}, \ell_1, \ell_2, \ell_3, \ell_4 \in \mathbb{Z}\}.$$

Then, \mathbb{B} is also described as the quotient group

$$\mathbb{B} = \mathbb{A}_4 / \langle \beta^2 \alpha_1^{-1} \alpha_2^{-1} \alpha_3^{-1} \rangle,$$

where $\langle \beta^2 \alpha_1^{-1} \alpha_2^{-1} \alpha_3^{-1} \rangle$ is the (normal) subgroup generated by $\beta^2 \alpha_1^{-1} \alpha_2^{-1} \alpha_3^{-1}$. We shall consider the group ring $\mathbb{C}[\mathbb{B}]$ of \mathbb{B} ,

$$\mathcal{R}_3 := \mathbb{C}[\mathbb{B}] = \mathbb{C}[\alpha_1, \alpha_2, \alpha_3, \alpha_1^{-1}, \alpha_2^{-1}, \alpha_3^{-1}, \beta, \beta^{-1}] / (\beta^2 - \alpha_1 \alpha_2 \alpha_3).$$

4.3. Fiber Structure of BCC Lattice. In this subsection, we consider a projection of the BCC lattice and its associated fibering structure.

As in the case of \mathcal{R}_d discussed in Subsection 4.1, let us consider

$$\mathbb{B}_d := \{(\alpha_1 \alpha_3^{-1})^{\ell_1} (\alpha_2 \alpha_3^{-1})^{\ell_2} \mid \ell_1, \ell_2 \in \mathbb{Z}\},$$

which is a subgroup of \mathbb{B} . Then, we have the following decomposition as a $\mathbb{C}[\mathbb{B}_d]$ -module.

Lemma 4.5. *We have a natural isomorphism as $\mathbb{C}[\mathbb{B}_d]$ -modules:*

$$\begin{aligned}\mathcal{R}_3 / (\alpha_1 \alpha_2 \alpha_3 - 1) &\cong \mathbb{C}[\mathbb{B}_d] \oplus \mathbb{C}[\mathbb{B}_d] \alpha_1 \oplus \mathbb{C}[\mathbb{B}_d] \alpha_1 \alpha_2 \\ &\quad \oplus \mathbb{C}[\mathbb{B}_d] \beta \oplus \mathbb{C}[\mathbb{B}_d] \alpha_1 \beta \oplus \mathbb{C}[\mathbb{B}_d] \alpha_1 \alpha_2 \beta.\end{aligned}$$

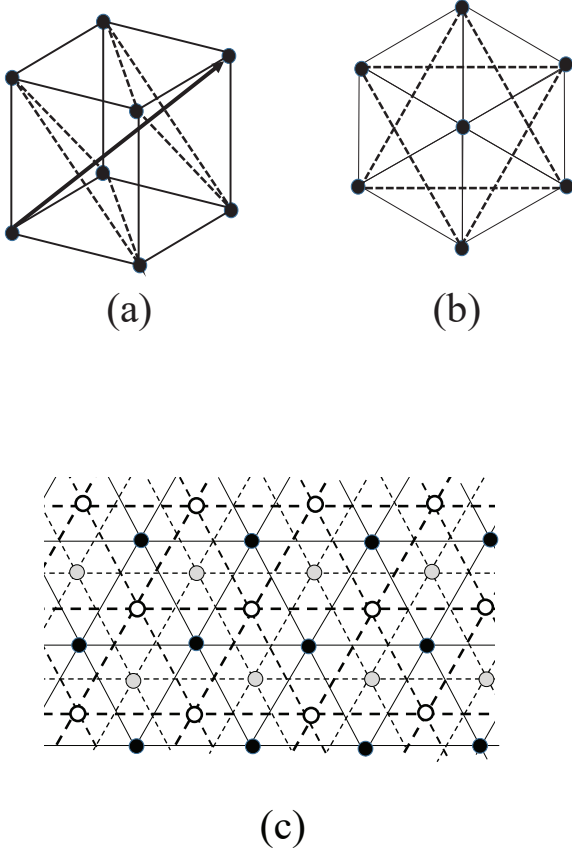


FIGURE 4. The cube in (a) shows the triangles whose normal direction is $(1, 1, 1)$ in simple cubic lattice. If one looks at the cube from the $(1, 1, 1)$ -direction, then the image is as in (b). Furthermore, if one projects the whole SC lattice to the plane perpendicular to the $(1, 1, 1)$ -direction, then one gets the image as in (c), where the black, gray and white dots correspond to the three sheets $\mathcal{A}_d^{(0)}$, $\mathcal{A}_d^{(1)}$ and $\mathcal{A}_d^{(2)}$.

We can prove the above lemma by using an argument similar to that in the proof of Lemma 4.1.

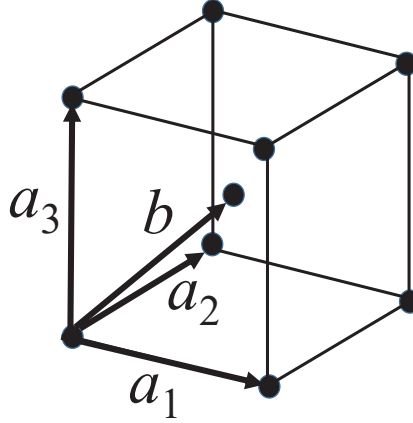


FIGURE 5. Body centered cubic (BCC) lattice

Remark 4.6. As in Remark 4.3, we can also prove Lemma 4.5 using the snake lemma [L] as follows. First, note that we have

$$\begin{aligned}
 & \mathcal{R}_3/(\alpha_1\alpha_2\alpha_3 - 1) \\
 \cong & \mathbb{C}[\alpha_1, \alpha_2, \alpha_3, \alpha_1^{-1}, \alpha_2^{-1}, \alpha_3^{-1}, \beta, \beta^{-1}]/(\beta^2 - \alpha_1\alpha_2\alpha_3, \alpha_1\alpha_2\alpha_3 - 1) \\
 \cong & \mathbb{C}[\alpha_1, \alpha_2, \alpha_3, \alpha_1^{-1}, \alpha_2^{-1}, \alpha_3^{-1}, \beta, \beta^{-1}]/(\beta^2 - 1, \alpha_1\alpha_2\alpha_3 - 1) \\
 \cong & \mathbb{C}[\alpha_1, \alpha_2, \alpha_3, \alpha_1^{-1}, \alpha_2^{-1}, \alpha_3^{-1}]/(\alpha_1\alpha_2\alpha_3 - 1) \oplus \mathbb{C}[\beta, \beta^{-1}]/(\beta^2 - 1).
 \end{aligned}$$

Using the additive version \mathbb{B}_d^a of the abelian multiplicative group \mathbb{B}_d , we have the commutative diagram with exact rows

$$\begin{array}{ccccccc}
 & & & \begin{pmatrix} 3 & 0 \\ 0 & 2 \end{pmatrix} & & & \\
 & & & \mathbb{Z}^2 & \xrightarrow{\quad} & 3\mathbb{Z} \oplus 2\mathbb{Z} & \longrightarrow 0 \\
 & & \begin{pmatrix} 1 & 0 \\ 1 & 0 \\ 1 & 0 \\ 0 & 2 \end{pmatrix} & \downarrow & \begin{pmatrix} 1 & 1 & 1 & 0 \\ 0 & 0 & 0 & 1 \end{pmatrix} & \downarrow & \\
 0 & \longrightarrow & \mathbb{B}_d^a & \longrightarrow & \mathbb{Z}^4 & \longrightarrow & \mathbb{Z}^2 \longrightarrow 0,
 \end{array}$$

where the rightmost vertical map and the second horizontal map in the lower sequence are the natural inclusions. By applying the snake lemma to this diagram, we obtain the relation in Lemma 4.5 as in Remark 4.3.

Thus, we have the following.

Proposition 4.7. *For*

$$\mathcal{R} := \mathcal{R}_3/(\beta - 1),$$

we have a natural isomorphism as $\mathbb{C}[\mathbb{B}_d]$ -modules:

$$\mathcal{R} \cong \mathbb{C}[\mathbb{B}_d] \oplus \mathbb{C}[\mathbb{B}_d]\alpha_1 \oplus \mathbb{C}[\mathbb{B}_d]\alpha_1\alpha_2.$$

Remark 4.8. This corresponds to the triangle diagram for the projection of the BCC lattice, which is, in fact, the same as that depicted in Figure 4 (c). For the screw dislocation in the BCC lattice, $b \in \mathbb{B}$ coincides with the associated Burgers vector $[N]$. In other words, geometrically the “base space” corresponds to three sheets if we consider them as embedded in \mathbb{E}^3 as shown in Figure 4. This comes from the discrete nature of the lattice. However, the interval between the sheets is now given by $\sqrt{3}a/6$, which differs from that in the SC lattice case. More precisely, let us denote by \mathcal{B} the subset of \mathbb{E}^3 corresponding to the three sheets. Then, we have

$$\mathcal{B} := \mathcal{B}^{(0)} \amalg \mathcal{B}^{(1)} \amalg \mathcal{B}^{(2)},$$

where

$$\begin{aligned} \mathcal{B}^{(0)} &:= \{\ell_1(a_1 - a_3) + \ell_2(a_2 - a_3) \mid \ell_1, \ell_2 \in \mathbb{Z}\}, \\ \mathcal{B}^{(1)} &:= \{\ell_1(a_1 - a_3) + \ell_2(a_2 - a_3) + a_1 - b \mid \ell_1, \ell_2 \in \mathbb{Z}\}, \\ \mathcal{B}^{(2)} &:= \{\ell_1(a_1 - a_3) + \ell_2(a_2 - a_3) + a_1 + a_2 - b \mid \ell_1, \ell_2 \in \mathbb{Z}\}. \end{aligned}$$

By observing that the degree of b is equal to $3/2$, we see that the three sheets above correspond to the classification by the degrees (modulo $3/2$).

Thus, we have the following.

Lemma 4.9. *As a set, \mathbb{B}^a is also decomposed as*

$$\mathbb{B}^a = \mathbb{B}^{(0)} \amalg \mathbb{B}^{(1)} \amalg \mathbb{B}^{(2)},$$

where

$$\begin{aligned} \mathbb{B}^{(0)} &:= \{\ell_1(a_1 - a_3) + \ell_2(a_2 - a_3) + \ell_3 b \mid \ell_1, \ell_2, \ell_3 \in \mathbb{Z}\}, \\ \mathbb{B}^{(1)} &:= \{\ell_1(a_1 - a_3) + \ell_2(a_2 - a_3) + a_1 + \ell_3 b \mid \ell_1, \ell_2, \ell_3 \in \mathbb{Z}\}, \\ \mathbb{B}^{(2)} &:= \{\ell_1(a_1 - a_3) + \ell_2(a_2 - a_3) + a_1 + a_2 + \ell_3 b \mid \ell_1, \ell_2, \ell_3 \in \mathbb{Z}\}. \end{aligned}$$

Let $\eta : \mathbb{R}^3 \rightarrow \mathbb{R}^3$ be the orthogonal transformation that sends a_1 , a_2 and a_3 to the vectors

$$a \begin{pmatrix} \sqrt{2}/2 \\ -\sqrt{6}/6 \\ \sqrt{3}/3 \end{pmatrix}, a \begin{pmatrix} 0 \\ \sqrt{6}/3 \\ \sqrt{3}/3 \end{pmatrix} \text{ and } a \begin{pmatrix} -\sqrt{2}/2 \\ -\sqrt{6}/6 \\ \sqrt{3}/3 \end{pmatrix},$$

respectively. For a vector $\delta = (\delta_1, \delta_2, \delta_3) \in \mathbb{E}^3$, we consider the embedding

$$\iota_\delta^{\text{BCC}} : \mathbb{B}^a \hookrightarrow \mathbb{E}^3$$

defined by $x \mapsto \eta(x) + \delta$ for $x \in \mathbb{B}^a \subset \mathbb{R}^3$. Note that η sends the vector $2b = a(1, 1, 1)$ to $\sqrt{3}a(0, 0, 1)$, and therefore $\iota_\delta^{\text{BCC}}$ sends each $\mathbb{B}^{(c)}$ into a plane parallel to the plane spanned by $(1, 0, 0)$ and $(0, 1, 0)$ for $c = 0, 1, 2$.

Let $\pi : \mathbb{E}^3 \rightarrow \mathbb{E}^2$ be the natural projection to the first and second coordinates. As in the case of \mathcal{A}_d , we consider the natural embedding $\iota_\delta^{\text{BCC}, c} = \pi \circ \iota_\delta^{\text{BCC}}|_{\mathcal{B}^{(c)}} : \mathcal{B}^{(c)} = \mathbb{Z}^2 \hookrightarrow \mathbb{E}^2$, $c = 0, 1, 2$.

With the help of Figure 6, we can prove the following lemma.

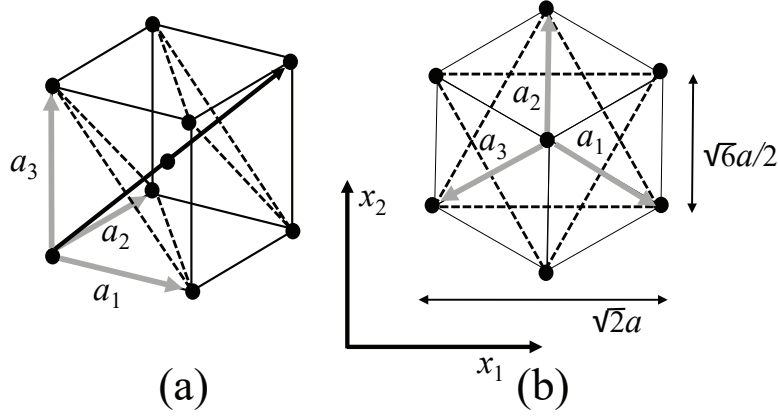


FIGURE 6. Body centered cubic lattice and its projection along the $(1, 1, 1)$ -direction

Lemma 4.10. *For the embedding $\iota_{\bar{\delta}}^{\text{BCC},c} : \mathcal{B}^{(c)} \hookrightarrow \mathbb{E}^2$, $c = 0, 1, 2$, we have the following:*

$$\begin{aligned} \iota_{\bar{\delta}}^{\text{BCC},0}(x) &= (\sqrt{2}\ell_1 a + \sqrt{2}\ell_2 a/2, \sqrt{6}\ell_2 a/2) \\ &\quad \text{for } x = \ell_1(a_1 - a_3) + \ell_2(a_2 - a_3) \in \mathcal{B}^{(0)}, \\ \iota_{\bar{\delta}}^{\text{BCC},1}(x) &= (\sqrt{2}\ell_1 a + \sqrt{2}a/2 + \sqrt{2}\ell_2 a/2, (\sqrt{6}\ell_2 a - \sqrt{6}a/3)/2) \\ &\quad \text{for } x = \ell_1(a_1 - a_3) + \ell_2(a_2 - a_3) + a_1 - b \in \mathcal{B}^{(1)}, \\ \iota_{\bar{\delta}}^{\text{BCC},2}(x) &= (\sqrt{2}\ell_1 a + \sqrt{2}a/2 + \sqrt{2}\ell_2 a/2, (\sqrt{6}\ell_2 a + 2\sqrt{6}a/3)/2) \\ &\quad \text{for } x = \ell_1(a_1 - a_3) + \ell_2(a_2 - a_3) + a_1 + a_2 - b \in \mathcal{B}^{(2)}. \end{aligned}$$

Let $\mathcal{S} = \mathcal{S}_+ \amalg \mathcal{S}_-$ be a finite subset in \mathbb{E}^2 as in Subsection 2.3. In the following, we assume that $\bar{\delta} \in \mathbb{E}^2$ satisfies $\iota_{\bar{\delta}}^{\text{BCC},c}(\mathcal{B}^{(c)}) \cap \mathcal{S} = \emptyset$, $c = 0, 1, 2$. Then, we have the following, whose proof is straightforward.

Lemma 4.11. *For every fiber bundle $F_{\mathbb{E}^2 \setminus \mathcal{S}}$ over $\mathbb{E}^2 \setminus \mathcal{S}$, by the embedding $\iota_{\bar{\delta}}^{\text{BCC},c} : \mathcal{B}^{(c)} \hookrightarrow \mathbb{E}^2 \setminus \mathcal{S}$, $c = 0, 1, 2$, we have the pullback bundle $F_{\mathcal{B}^{(c)}}$ that satisfies the commutative diagram*

$$\begin{array}{ccc} F_{\mathcal{B}^{(c)}} & \xrightarrow{\iota_{\bar{\delta}}^{\text{BCC},c}} & F_{\mathbb{E}^2 \setminus \mathcal{S}} \\ \downarrow & & \downarrow \\ \mathcal{B}^{(c)} & \xrightarrow{\iota_{\bar{\delta}}^{\text{BCC},c}} & \mathbb{E}^2 \setminus \mathcal{S}, \end{array}$$

where the vertical maps are the projections of the fiber bundles and $\hat{\iota}_{\bar{\delta}}^{\text{BCC},c}$ is the bundle map induced by $\iota_{\bar{\delta}}^{\text{BCC},c}$.

Using this pullback diagram (Cartesian square), we have the following, whose proof is straightforward.

Lemma 4.12. *We have the following commutative diagram:*

$$\begin{array}{ccc}
 \mathbb{E}_{\mathcal{B}^{(c)}} & \xrightarrow{\hat{\iota}_{\delta}^{\text{BCC},c}} & \mathbb{E}_{\mathbb{E}^2 \setminus \mathcal{S}} \\
 \downarrow & & \downarrow \\
 \mathcal{B}^{(c)} & \xrightarrow{\iota_{\delta}^{\text{BCC},c}} & \mathbb{E}^2 \setminus \mathcal{S} \\
 \uparrow & & \uparrow \\
 S_{\mathcal{B}^{(c)}}^1 & \xrightarrow{\hat{\iota}_{\delta}^{\text{BCC},c}} & S_{\mathbb{E}^2 \setminus \mathcal{S}}^1
 \end{array}
 \begin{array}{c}
 \widehat{\psi} \\
 \left. \begin{array}{c} \curvearrowright \\ \curvearrowleft \end{array} \right\} \\
 \widehat{\psi}
 \end{array}$$

for $c = 0, 1, 2$, where the straight vertical arrows are projections of the fiber bundles, $\widehat{\psi}$ are the bundle maps induced by ψ defined in Section 2, and the positive constant d in Section 2 is now set $d = \sqrt{3}a/2$, which $\widehat{\psi}$ depends on.

The following proposition corresponds to the case where $\mathcal{S} = \emptyset$ and the proof is left to the reader.

Proposition 4.13. *Set $\gamma = \exp(4\pi\sqrt{-1}\delta_3/(\sqrt{3}a)) \in S^1$ and consider the global sections*

$$\check{\sigma}_{\gamma,c} \in \Gamma(\mathcal{B}^{(c)}, S_{\mathcal{B}^{(c)}}^1), \quad c = 0, 1, 2,$$

that constantly take the values $\gamma\zeta_3^{-c}$, where $\zeta_3 = \exp(2\pi\sqrt{-1}/3)$. Then, we have

$$\hat{\iota}_{\delta}^{\text{BCC}}(\mathbb{B}^a) = \bigcup_{c=0}^2 \hat{\iota}_{\delta}^{\text{BCC},c} \left(\widehat{\psi}^{-1}(\check{\sigma}_{\gamma,c}(\mathcal{B}^{(c)})) \right) \subset \mathbb{E}^3.$$

4.4. Algebraic Description of Screw Dislocations in BCC Lattice. Recall that a screw dislocation in the BCC lattice is basically given by the $(1, 1, 1)$ -direction. In other words, the Burgers vector is parallel to the $(1, 1, 1)$ -direction, or more precisely it coincides with b itself [N].

In the following, for $\gamma' \in S^1$ and $\check{\sigma} \in \Gamma(\mathcal{B}, S_{\mathcal{B}}^1)$ expressed as $\check{\sigma}(x) = (s(x), x)$ for $x \in \mathcal{B}$, we define their multiplication $\gamma'\check{\sigma} \in \Gamma(\mathcal{B}, S_{\mathcal{B}}^1)$ by $(\gamma'\check{\sigma})(x) = (\gamma's(x), x)$, $x \in \mathcal{B}$.

Now, as in Proposition 3.6 for the SC lattice case, we have the following description of a single screw dislocation in the BCC lattice.

Proposition 4.14. *The single screw dislocation expressed by*

$$\bigcup_{c=0}^2 \hat{\iota}_{\delta}^{\text{BCC},c} \left(\widehat{\psi}^{-1} \left((\gamma\zeta_3^{-c}\check{\sigma}_{z_0})(\mathcal{B}^{(c)}) \right) \right)$$

around $z_0 \in \mathbb{E}^2$ is a subset of \mathbb{E}^3 , where $\check{\sigma}_{z_0}$ is an element of $\Gamma(\mathcal{B}, S_{\mathcal{B}}^1)$ given by

$$\check{\sigma}_{z_0}(x) = \left(\frac{\sqrt{2}\ell_1 a + \sqrt{2}\ell_2 a/2 - x_0 + \sqrt{-1}(\sqrt{6}\ell_2 a/2 - y_0)}{|\sqrt{2}\ell_1 a + \sqrt{2}\ell_2 a/2 - x_0 + \sqrt{-1}(\sqrt{6}\ell_2 a/2 - y_0)|}, x \right) \\ \text{for } x = \ell_1(a_1 - a_3) + \ell_2(a_2 - a_3) \in \mathcal{B}^{(0)},$$

$$\check{\sigma}_{z_0}(x) = \left(\frac{\sqrt{2}\ell_1 a + \sqrt{2}a/2 + \sqrt{2}\ell_2 a/2 - x_0 + \sqrt{-1}((\sqrt{6}\ell_2 a - \sqrt{6}a/3)/2 - y_0)}{|\sqrt{2}\ell_1 a + \sqrt{2}a/2 + \sqrt{2}\ell_2 a/2 - x_0 + \sqrt{-1}((\sqrt{6}\ell_2 a - \sqrt{6}a/3)/2 - y_0)|}, x \right) \\ \text{for } x = \ell_1(a_1 - a_3) + \ell_2(a_2 - a_3) + a_1 - b \in \mathcal{B}^{(1)},$$

$$\check{\sigma}_{z_0}(x) = \left(\frac{\sqrt{2}\ell_1 a + \sqrt{2}a/2 + \sqrt{2}\ell_2 a/2 - x_0 + \sqrt{-1}((\sqrt{6}\ell_2 a + 2\sqrt{6}a/3)/2 - y_0)}{|\sqrt{2}\ell_1 a + \sqrt{2}a/2 + \sqrt{2}\ell_2 a/2 - x_0 + \sqrt{-1}((\sqrt{6}\ell_2 a + 2\sqrt{6}a/3)/2 - y_0)|}, x \right) \\ \text{for } x = \ell_1(a_1 - a_3) + \ell_2(a_2 - a_3) + a_1 + a_2 - b \in \mathcal{B}^{(2)},$$

where $z_0 = x_0 + \sqrt{-1}y_0 \in \mathbb{C}$ and $(\ell_1, \ell_2) \in \mathbb{Z}^2$.

Furthermore, for $\check{\sigma}_1$ and $\check{\sigma}_2 \in \Gamma(\mathcal{B}, S_{\mathcal{B}}^1)$ expressed as $\check{\sigma}_a(x) = (s_a(x), x)$ for $x \in \mathcal{B}$, $a = 1, 2$, we define their multiplication $\check{\sigma}_1\check{\sigma}_2$ by $(\check{\sigma}_1\check{\sigma}_2)(x) = (s_1(x)s_2(x), x)$, $x \in \mathcal{B}$. Using the multiplication, we have the following description of a parallel multi-screw dislocation in the BCC lattice.

Proposition 4.15. *The parallel multi-screw dislocation in the BCC lattice given by*

$$\bigcup_{c=0}^2 \hat{\iota}_{\check{\delta}}^{\text{BCC},c} \left(\hat{\psi}^{-1} \left(\left(\gamma\zeta_3^{-c} \prod_{z_i \in \mathcal{S}_+} \check{\sigma}_{z_i} \prod_{z_j \in \mathcal{S}_-} \check{\sigma}_{z_j} \right) (\mathcal{B}^{(c)}) \right) \right) \\ = \bigcup_{c=0}^2 \hat{\iota}_{\check{\delta}}^{\text{BCC},c} \left(\frac{\sqrt{3}a}{12\pi\sqrt{-1}} \exp^{-1} \left(\left(\gamma\zeta_3^{-c} \prod_{z_i \in \mathcal{S}_+} \check{\sigma}_{z_i} \prod_{z_j \in \mathcal{S}_-} \check{\sigma}_{z_j} \right) (\mathcal{B}^{(c)}) \right) \right)$$

is a subset of \mathbb{E}^3 , where \mathcal{S} corresponds to the position of the dislocation lines.

5. ENERGY OF SCREW DISLOCATION

5.1. Energy of Screw Dislocation in SC Lattice. In this section, we consider the strain energy of a single screw dislocation in the SC lattice along the $(0, 0, 1)$ -direction as discussed in Subsection 3.3. We adopt a spring model, in which certain “edges” of the SC lattice correspond to elastic springs, whose natural lengths are equal to a or $\sqrt{2}a$.

More precisely, in our model, we have the elastic springs on the edges

$$[(\ell_1, \ell_2, \ell_3), (\ell_1 + 1, \ell_2, \ell_3)], \quad [(\ell_1, \ell_2, \ell_3), (\ell_1, \ell_2 + 1, \ell_3)],$$

$$\begin{aligned}
 & [(\ell_1, \ell_2, \ell_3), (\ell_1, \ell_2, \ell_3 + 1)], \quad [(\ell_1, \ell_2, \ell_3), (\ell_1 + 1, \ell_2, \ell_3 \pm 1)], \\
 & [(\ell_1, \ell_2, \ell_3), (\ell_1, \ell_2 + 1, \ell_3 \pm 1)], \quad [(\ell_1, \ell_2, \ell_3), (\ell_1 + 1, \ell_2 \pm 1, \ell_3)],
 \end{aligned}$$

for all $(\ell_1, \ell_2, \ell_3) \in \mathbb{Z}^3$. Note that the above parametrization refers to a local one for the SC lattice after the dislocation, in a neighborhood of each vertex sufficiently far from the dislocation line. It is clear that such a parametrization does not work globally; however, around each point, such a parametrization works as long as the point is far from the dislocation center. In this section we will use this parameterization for simplicity and compute the strain energy caused by a screw dislocation.

We note that there are several other possibilities for the choice of the edges. The choice of the model, however, does not affect the essentials of the results, as we will see later.

Now, let us consider the screw dislocation in the SC lattice along the $(0, 0, 1)$ -direction around $z_0 \in \mathbb{C}$, as described in Subsection 3.3. We regard that the original lattice is in a stable position, and we consider the elastic energy resulting from the dislocation. For this, we need to investigate the difference between the original position and the position resulting from the dislocation.

First, we define the relative height difference $\epsilon_{\ell_1, \ell_2}^{(1)}$, $\epsilon_{\ell_1, \ell_2}^{(2)}$ and $\epsilon_{\ell_1, \ell_2}^{(\pm)}$ by

$$\begin{aligned}
 (5.1) \quad \epsilon_{\ell_1, \ell_2}^{(1)} &= \frac{a}{2\pi\sqrt{-1}} (\log(\check{\sigma}_{z_0, \gamma}(\ell_1 + 1, \ell_2)) - \log(\check{\sigma}_{z_0, \gamma}(\ell_1, \ell_2))), \\
 \epsilon_{\ell_1, \ell_2}^{(2)} &= \frac{a}{2\pi\sqrt{-1}} (\log(\check{\sigma}_{z_0, \gamma}(\ell_1, \ell_2 + 1)) - \log(\check{\sigma}_{z_0, \gamma}(\ell_1, \ell_2))), \\
 \epsilon_{\ell_1, \ell_2}^{(\pm)} &= \frac{a}{2\pi\sqrt{-1}} (\log(\check{\sigma}_{z_0, \gamma}(\ell_1 + 1, \ell_2 \pm 1)) - \log(\check{\sigma}_{z_0, \gamma}(\ell_1, \ell_2))),
 \end{aligned}$$

respectively, where $\log x = \log_e x$ for $x \in S^1$ is considered to be $\sqrt{-1}$ times the argument of x , and we choose the values so that $-a/2 < \epsilon_{\ell_1, \ell_2}^{(i)} < a/2$ for $i = 1, 2$ and \pm .

In what follows, for a section $\check{\sigma} \in \Gamma(\mathcal{A}_p, S_{\mathcal{A}_p}^1)$ expressed as $\check{\sigma}(x) = (s(x), x)$ for $x \in \mathcal{A}_p$, we often use the symbol $\check{\sigma}(x)$ instead of $s(x)$ by abuse of notation. We recall that

$$\check{\sigma}_{z_0}(\ell_1 a, \ell_2 a) = \check{\sigma}_{z_0, \gamma}(\ell_1 a, \ell_2 a) = \frac{\ell_1 a - x_0 + \sqrt{-1}(\ell_2 a - y_0)}{|\ell_1 a - x_0 + \sqrt{-1}(\ell_2 a - y_0)|}$$

for $z_0 = x_0 + \sqrt{-1}y_0$, $x_0, y_0 \in \mathbb{R}$, and $\gamma = 1$ in Proposition 3.6.

Then, the difference of length in each segment

$$[(\ell_1, \ell_2, \ell_3), (\ell_1 + 1, \ell_2, \ell_3)] \quad \text{or} \quad [(\ell_1, \ell_2, \ell_3), (\ell_1, \ell_2 + 1, \ell_3)]$$

is given by

$$\Delta_{\ell_1, \ell_2}^{(i)} = \sqrt{a^2 + (\epsilon_{\ell_1, \ell_2}^{(i)})^2} - a,$$

$i = 1, 2$, whereas the difference of length in each diagonal segment

$$[(\ell_1, \ell_2, \ell_3), (\ell_1 + 1, \ell_2, \ell_3 \pm 1)] \quad \text{or} \quad [(\ell_1, \ell_2, \ell_3), (\ell_1, \ell_2 + 1, \ell_3 \pm 1)]$$

is given by

$$(5.2) \quad \Delta_{\ell_1, \ell_2}^{d(i, \pm)} = \sqrt{(a \pm \epsilon_{\ell_1, \ell_2}^{(i)})^2 + a^2} - \sqrt{2}a,$$

$i = 1, 2$, and the difference of length in the diagonal segment

$$[(\ell_1, \ell_2, \ell_3), (\ell_1 + 1, \ell_2 \pm 1, \ell_3)]$$

is given by

$$(5.3) \quad \Delta_{\ell_1, \ell_2}^{d(\pm)} = \sqrt{2a^2 + (\epsilon_{\ell_1, \ell_2}^{(\pm)})^2} - \sqrt{2}a.$$

On the other hand, the length of the segment $[(\ell_1, \ell_2, \ell_3), (\ell_1, \ell_2, \ell_3 + 1)]$ is constantly equal to the natural length a and thus we set $\Delta_{\ell_1, \ell_2}^{(3)} = 0$.

Then, we have the following.

Lemma 5.1. *If*

$$\frac{a}{\sqrt{(\ell_1 a - x_0)^2 + (\ell_2 a - y_0)^2}}$$

is sufficiently small, then $\epsilon_{\ell_1, \ell_2}^{(1)}$, $\epsilon_{\ell_1, \ell_2}^{(2)}$ and $\epsilon_{\ell_1, \ell_2}^{(\pm)}$ are approximately given by

$$(5.4) \quad \begin{aligned} \epsilon_{\ell_1, \ell_2}^{(1)} &= -\frac{a}{2\pi} \frac{a(\ell_2 a - y_0)}{(\ell_1 a - x_0)^2 + (\ell_2 a - y_0)^2} \\ &\quad + o\left(\frac{a}{\sqrt{(\ell_1 a - x_0)^2 + (\ell_2 a - y_0)^2}}\right), \\ \epsilon_{\ell_1, \ell_2}^{(2)} &= -\frac{a}{2\pi} \frac{a(\ell_1 a - x_0)}{(\ell_1 a - x_0)^2 + (\ell_2 a - y_0)^2} \\ &\quad + o\left(\frac{a}{\sqrt{(\ell_1 a - x_0)^2 + (\ell_2 a - y_0)^2}}\right), \\ \epsilon_{\ell_1, \ell_2}^{(\pm)} &= -\frac{a}{2\pi} \frac{\pm a(\ell_1 a - x_0) + a(\ell_2 a - y_0)}{(\ell_1 a - x_0)^2 + (\ell_2 a - y_0)^2} \\ &\quad + o\left(\frac{a}{\sqrt{(\ell_1 a - x_0)^2 + (\ell_2 a - y_0)^2}}\right), \end{aligned}$$

respectively, whereas $\Delta_{\ell_1, \ell_2}^{(i)}$, $\Delta_{\ell_1, \ell_2}^{d(i, \pm)}$ and $\Delta_{\ell_1, \ell_2}^{d(\pm)}$ are approximately given by

$$(5.5) \quad \begin{aligned} \Delta_{\ell_1, \ell_2}^{(i)} &= \frac{1}{2a} (\epsilon_{\ell_1, \ell_2}^{(i)})^2 + o\left(\frac{a}{\sqrt{(\ell_1 a - x_0)^2 + (\ell_2 a - y_0)^2}}\right), \\ \Delta_{\ell_1, \ell_2}^{d(i, \pm)} &= \pm \frac{1}{\sqrt{2}} \epsilon_{\ell_1, \ell_2}^{(i)} + o\left(\frac{a}{\sqrt{(\ell_1 a - x_0)^2 + (\ell_2 a - y_0)^2}}\right), \\ \Delta_{\ell_1, \ell_2}^{d(\pm)} &= \frac{1}{2\sqrt{2}a} (\epsilon_{\ell_1, \ell_2}^{(\pm)})^2 + o\left(\frac{a}{\sqrt{(\ell_1 a - x_0)^2 + (\ell_2 a - y_0)^2}}\right), \end{aligned}$$

respectively, $i = 1, 2$.

Proof. For simplicity, we set

$$z := (\ell_1 a - x_0) + \sqrt{-1}(\ell_2 a - y_0).$$

Then, we have

$$\begin{aligned} \check{\sigma}_{z_0}((\ell_1 + 1)a, \ell_2 a) &= \frac{z + a}{|z + a|} = \check{\sigma}_{z_0}(\ell_1 a, \ell_2 a) \frac{1 + a/z}{|1 + a/z|}, \\ \check{\sigma}_{z_0}(\ell_1 a, (\ell_2 + 1)a) &= \frac{z + \sqrt{-1}a}{|z + \sqrt{-1}a|} = \check{\sigma}_{z_0}(\ell_1 a, \ell_2 a) \frac{1 + \sqrt{-1}a/z}{|1 + \sqrt{-1}a/z|}, \\ \check{\sigma}_{z_0}((\ell_1 + 1)a, (\ell_2 \pm 1)a) &= \frac{z + a \pm \sqrt{-1}a}{|z + a \pm \sqrt{-1}a|} \\ &= \check{\sigma}_{z_0}(\ell_1 a, \ell_2 a) \frac{1 + (a \pm \sqrt{-1}a)/z}{|1 + (a \pm \sqrt{-1}a)/z|}. \end{aligned}$$

By Taylor expansion, we have, for $w = \xi + \sqrt{-1}\xi'$, $\xi, \xi' \in \mathbb{R}$,

$$\arg(1 + w) = \arctan \frac{\xi'}{1 + \xi} = \xi' + o(|w|)$$

as $w \rightarrow 0$. Therefore, we obtain that

$$\begin{aligned}
 \arg\left(1 + \frac{a}{z}\right) &= \operatorname{Im} \frac{a}{z} + o\left(\frac{a}{|z|}\right) \\
 &= -\frac{a}{|z|^2}(\ell_2 a - y_0) + o\left(\frac{a}{|z|}\right), \\
 \arg\left(1 + \frac{\sqrt{-1}a}{z}\right) &= \operatorname{Re} \frac{a}{z} + o\left(\frac{a}{|z|}\right) \\
 &= \frac{a}{|z|^2}(\ell_1 a - x_0) + o\left(\frac{a}{|z|}\right), \\
 \arg\left(1 + \frac{(a \pm \sqrt{-1}a)}{z}\right) &= \operatorname{Im} \frac{a}{z} \pm \operatorname{Re} \frac{a}{z} + o\left(\frac{a}{|z|}\right) \\
 &= \frac{a}{|z|^2}(-(\ell_2 a - y_0) \pm (\ell_1 a - x_0)) + o\left(\frac{a}{|z|}\right).
 \end{aligned}$$

Then, we get the approximation formula (5.4) from definition (5.1).

Finally, we can prove the approximation formula (5.5) for $\Delta_{\ell_1, \ell_2}^{(i)}$, $\Delta_{\ell_1, \ell_2}^{d(i, \pm)}$, $i = 1, 2$, and $\Delta_{\ell_1, \ell_2}^{d(\pm)}$ by simple application of the Taylor expansion. This completes the proof. \square

Following the spirit of the theory of elasticity [LL, M], in the following, we assume that

$$\frac{a}{\sqrt{(a\ell_1 - x_0)^2 + (a\ell_2 - y_0)^2}}$$

is small in Lemma 5.1. This assumption means that the node $(\ell_1 a, \ell_2 a)$ in \mathbb{E}^2 is sufficiently far from the center (x_0, y_0) of dislocation relative to the lattice length a . Such an approximation does not hold for the nodes near the center. More explicitly, the approximation given above is valid for the elastic energy in the far region

$$(5.6) \quad A_\rho := \left\{ (\ell_1, \ell_2) \in \mathbb{Z}^2 \mid \rho a < \sqrt{(\ell_1 a - x_0)^2 + (\ell_2 a - y_0)^2} \right\}$$

for sufficiently large fixed $\rho > 0$. On the other hand, in the core region $\mathbb{Z}^2 \setminus A_\rho$, the approximation fails and we need to adopt another approach.

Furthermore, for later convenience, let us introduce the notation

$$(5.7) \quad A_{\rho, N} := \left\{ (\ell_1, \ell_2) \in \mathbb{Z}^2 \mid \rho a < \sqrt{(\ell_1 a - x_0)^2 + (\ell_2 a - y_0)^2} < Na \right\}$$

for $N > \rho$, which is bounded and is a finite set.

We can now compute the elastic energy caused by the screw dislocation. Since our model has the translational symmetry along the $(0, 0, 1)$ -axis (i.e., the set of lattice points (ℓ_1, ℓ_2, ℓ_3) together with the edges with springs in our model is invariant under the translation $\ell_3 \mapsto \ell_3 + 1$), we will concentrate ourselves on the energy density for unit length in the $(0, 0, 1)$ -direction, and call it simply the elastic energy of dislocation again.

Let k_p and k_d be spring constants of the horizontal springs and the diagonal springs, respectively. Then, the elastic energy of dislocation in the annulus region $A_{\rho, N}$ is given

by

$$\begin{aligned}
E_{\rho,N}(x_0, y_0) &:= \sum_{(\ell_1, \ell_2) \in A_{\rho,N}} \left(\frac{1}{2} k_p \left(\left(\Delta_{\ell_1, \ell_2}^{(1)} \right)^2 + \left(\Delta_{\ell_1, \ell_2}^{(2)} \right)^2 + \left(\Delta_{\ell_1, \ell_2}^{(3)} \right)^2 \right) \right. \\
&\quad \left. + \frac{1}{2} k_d \left(\left(\Delta_{\ell_1, \ell_2}^{d(1,+)} \right)^2 + \left(\Delta_{\ell_1, \ell_2}^{d(2,+)} \right)^2 + \left(\Delta_{\ell_1, \ell_2}^{d(1,-)} \right)^2 \right. \right. \\
&\quad \left. \left. + \left(\Delta_{\ell_1, \ell_2}^{d(2,-)} \right)^2 + \left(\Delta_{\ell_1, \ell_2}^{d(+)} \right)^2 + \left(\Delta_{\ell_1, \ell_2}^{d(-)} \right)^2 \right) \right) \\
&= k_d \sum_{(\ell_1, \ell_2) \in A_{\rho,N}} \left(\frac{1}{2} (\epsilon_{\ell_1, \ell_2}^{(1)})^2 + \frac{1}{2} (\epsilon_{\ell_1, \ell_2}^{(2)})^2 \right) \\
&\quad + o \left(\frac{a^2}{(\ell_1 a - x_0)^2 + (\ell_2 a - y_0)^2} \right) \\
&= \frac{1}{8\pi^2} k_d a^2 \sum_{(\ell_1, \ell_2) \in A_{\rho,N}} \frac{a^2}{(\ell_1 a - x_0)^2 + (\ell_2 a - y_0)^2} \\
&\quad + o \left(\frac{a^2}{(\ell_1 a - x_0)^2 + (\ell_2 a - y_0)^2} \right). \tag{5.8}
\end{aligned}$$

Now defining the *truncated Epstein-Hurwitz zeta function* $\zeta_{\rho,N}(s, z_0)$ as

$$\zeta_{\rho,N}(s, z_0) := \sum_{(\ell_1, \ell_2) \in A_{\rho,N}} \frac{1}{((\ell_1 + x_0)^2 + (\ell_2 + y_0)^2)^{s/2}}, \tag{5.9}$$

we have the following theorem for the elastic energy.

Theorem 5.2. *By neglecting the second and higher orders of*

$$\frac{a^2}{(\ell_1 a - x_0)^2 + (\ell_2 a - y_0)^2},$$

we have that the elastic energy is given by

$$E_{\rho,N}(x_0, y_0) = \frac{1}{8\pi^2} k_d a^2 \zeta_{\rho,N}(2, -z_0/a). \tag{5.10}$$

6. SUMMARY AND DISCUSSION

In this section, we provide summary and discussion of our results from physical viewpoints as well as from mathematical viewpoints. While this section is mainly for readers with background in physics, we also give some remarks from mathematical viewpoints as well.

We have described multiple screw dislocations that are parallel to each other in the continuum picture in Section 2 as in Definition 2.5, using the section of a certain S^1 -bundle as defined in (2.5). Although they were known as topological defects in [HB, N], in Proposition 2.6 we have shown that they are also expressed as a quotient space of the path space or as an abelian covering of $\mathbb{E}^2 \setminus \mathcal{S}$. This means that our screw dislocations are regarded as realizations of the abelian covering of $\mathbb{E}^2 \setminus \mathcal{S}$ in the euclidean three space \mathbb{E}^3 .

In Proposition 3.8 of Section 3, the discrete picture of such multiple screw dislocations in the SC lattice has been obtained as the pullback of the fiber structure of the multiple screw dislocations in the continuum picture. It can naturally be extended to the case of the BCC lattice. However, in the case of the BCC lattice, the Burgers vector is given by $(1, 1, 1)$ and its geometrical structure is a little bit complicated. In Section 4, in order to treat the BCC case, we expressed the fiber structure with respect to the $(1, 1, 1)$ -direction using algebraic methods. The geometrical properties are determined by purely algebraic computations as in Lemma 4.1 and Proposition 4.7. Apparently, such algebraic methods can be applied to more general settings.

In Section 5, we have computed the energy of a screw dislocation. This is, in fact, related to harmonic map theory as follows. The complete SC lattice is realized as the embedding $\iota_{\mathbb{A}_3, \delta} : \mathbb{A}_3^a (\cong \mathbb{Z}^3) \rightarrow \mathbb{E}^3$ as in (3.1). Such embeddings are parametrized by $\delta \in \mathbb{E}^3$, which can actually be considered to be elements of the 3-torus group $T^3 = \mathbb{R}^3 / a\mathbb{Z}^3$. This is because if $\delta - \delta' \in a\mathbb{Z}^3$ for $\delta, \delta' \in \mathbb{E}^3$, then the images of $\iota_{\mathbb{A}_3, \delta}$ and $\iota_{\mathbb{A}_3, \delta'}$ coincide. Thus, a slight perturbation of the embedding $\iota_{\mathbb{A}_3, \delta}$ gives rise to a map $\mathbb{A}_3^a \rightarrow T^3$, and its infinitesimal version gives a map into the tangent space of T^3 , which is identified with \mathbb{R}^3 . Therefore, we can regard a realization of the lattice \mathbb{A}_3^a as a minimal point of a certain energy functional related to a harmonic map whose target space is T^3 , and we see that such an energy functional is given by our spring model by imitating the standard energy functional as introduced in [ES, U] from a discrete point of view.

On the other hand, a screw dislocation loses the symmetry except for the third axis. The fiber structure that we have discussed is related to the action of the subgroup $S^1 = \{1\} \times \{1\} \times S^1$ of T^3 . The configuration of a dislocation can also be regarded as a minimal point of an energy functional. Since the relevant map in the harmonic map theory for the dislocations is from $\mathcal{D}_S^{\text{SC}}$ to T^3 and S^1 acts on $\mathcal{D}_S^{\text{SC}}$, in Section 5 we have computed the energy of a screw dislocation by summing up the energy densities parametrized by $(\ell_1, \ell_2) \in \mathbb{Z}^2 \cong \mathcal{A}_p = \pi_{\mathcal{S}, \gamma}(\mathcal{D}_S^{\text{SC}})$, where $\pi_{\mathcal{S}, \gamma}$ is given in Definition 2.5.

Then, such an energy is approximately obtained in terms of the truncated Epstein-Hurwitz zeta function (5.9) in Theorem 5.2, where the Epstein-Hurwitz zeta function is defined by [Ep, El, T] as

$$(6.1) \quad \zeta(s, z_0) = \sum_{(\ell_1, \ell_2) \in \mathbb{Z}^2} \frac{1}{((\ell_1 + x_0)^2 + (\ell_2 + y_0)^2)^{s/2}}$$

for $z_0 = x_0 + \sqrt{-1}y_0$. Note that the zeta function diverges at $s = 2$, which implies that the elastic energy $E_{\rho,N}(x_0, y_0)$, approximately described in Theorem 5.2, diverges for $N \rightarrow \infty$, i.e.,

$$E_{\rho,N}(x_0, y_0) \rightarrow \infty, \quad \text{for } N \rightarrow \infty.$$

To study the dependence of $\zeta(s, z_0)$ on z_0 is a very important problem as the Hurwitz zeta function

$$\zeta(s, q) := \sum_{n=0}^{\infty} (n+q)^{-s}$$

has an interesting dependence on q . For example, the difference $\zeta(s, -z_0/a) - \zeta(s, -z'_0/a)$ for $z_0, z'_0 \in \mathbb{C}$ with $z_0 \neq z'_0$ is related to the elastic energy of our model. It should be noted, at least, that if $z'_0 - z_0$ is a lattice point of $a\mathbb{Z}^2$, then the difference must vanish.

Since the Epstein-Hurwitz zeta function is based on the theory of quadratic forms in euclidean spaces and the study of Minkowski [Ca], this fact might shed light on new mathematical aspects of the lattice theory besides [CS]. Furthermore, since the SC lattice \mathbb{A}_2^a can be regarded as the Gauss integers $\mathbb{Z}[\sqrt{-1}]$, these results might also reveal an important connection between the number theory and the theory of dislocations.

In this subsection, we summarize our results for physicists without mathematical rigourousness. We loosely use the logarithm function as a multiple valued function.

The results in Section 2 are basically well-known, e.g., in [HB, Chap. 4]. Let us consider multi-screw dislocations, whose dislocation lines are all parallel to the x_3 -direction and are given by points z_i in \mathcal{S}_+ for “positive” screw directions, and by points z_j in \mathcal{S}_- for “negative” ones, where \mathcal{S}_+ and \mathcal{S}_- are disjoint finite subsets of the complex plane \mathbb{C} . Set $\mathcal{S} = \mathcal{S}_+ \cup \mathcal{S}_-$. Setting the lattice unit d , we have seen that the x_3 -coordinates of the points in the dislocations are given by

$$(6.2) \quad \frac{d}{2\pi\sqrt{-1}} \log \left(\gamma \prod_{z_i \in \mathcal{S}_+} \frac{z - z_i}{|z - z_i|} \cdot \prod_{z_j \in \mathcal{S}_-} \frac{\overline{z - z_j}}{|z - z_j|} \right) \quad \text{for } z \in \mathbb{E}^2 \setminus \mathcal{S} = \mathbb{C} \setminus \mathcal{S}$$

for some $\gamma \in S^1$, where $\overline{z - z_j}$ is the complex conjugate of $z - z_j$. It consists of solutions to the Laplace equations

$$(6.3) \quad \frac{\partial}{\partial \bar{z}} \frac{\partial}{\partial z} \log \frac{z - z_k}{|z - z_k|} = 0 \quad \text{on } z \in \mathbb{C} \setminus \mathcal{S},$$

for $z_k \in \mathcal{S}$. In other words, the dislocations are obtained as a set of minimal points of the elastic energy under a certain boundary condition [HB, N].

Based on the result (6.2) in Section 2, we have described the discrete picture of the dislocation in the SC lattice in Subsection 3.3; at a point (ℓ_1, ℓ_2) of $\mathbb{Z}^2 \subset \mathbb{C}$, the lattice points are given by

$$\left(\ell_1 a, \ell_2 a, \frac{a}{2\pi\sqrt{-1}} \log \left(\gamma \prod_{z_i \in \mathcal{S}_+} \frac{(\ell_1 a + \ell_2 a \sqrt{-1}) - z_i}{|(\ell_1 a + \ell_2 a \sqrt{-1}) - z_i|} \prod_{z_j \in \mathcal{S}_-} \frac{\overline{(\ell_1 a + \ell_2 a \sqrt{-1}) - z_j}}{|(\ell_1 a + \ell_2 a \sqrt{-1}) - z_j|} \right) \right),$$

$(\ell_1 a, \ell_2 a) \in \mathcal{A}_p.$

These are realized as points in the configuration of the continuum picture. In other words, these are also based on the solutions to the Laplace equation (6.3).

For the BCC case, the dislocation layers are split into three types. Usually, the configuration has been discussed geometrically; however, in this article, we have shown the fact by means of an algebraic method. Experimentally, it is known that a dislocation line in a real material may not be a straight line, but is a curve in the 3-dimensional euclidean space \mathbb{E}^3 [HB]. Thus, we need to deal with such a curved dislocation line mathematically. Our algebraic approach might enable us to handle such a curve in a lattice locally which could be a part of a curved dislocation line. We should emphasize that our method is novel in this field of study.

Using the result (6.2) in Section 2, we have described the discrete picture of the dislocation in the BCC lattice in Subsection 4.4. Since we have shown it in Proposition 4.15

directly, let us rewrite it only for a single screw dislocation here:

The first layer:

$$\left(\sqrt{2}\ell_1 a + \sqrt{2}\ell_2 a/2, \sqrt{6}\ell_2 a/2, \frac{\sqrt{3}a}{2\pi\sqrt{-1}} \log \frac{L_0}{|L_0|} \right)$$

with $L_0 = \sqrt{2}\ell_1 a + \sqrt{2}\ell_2 a/2 - x_0 + \sqrt{-1}(\sqrt{6}\ell_2 a/2 - y_0)$
for $x = \ell_1(a_1 - a_3) + \ell_2(a_2 - a_3) \in \mathcal{B}^{(0)}$,

The second layer:

$$\left(\sqrt{2}\ell_1 a + \sqrt{2}a/2 + \sqrt{2}\ell_2 a/2, (\sqrt{6}\ell_2 a + 2\sqrt{6}a/3)/2, \right.$$

$$\left. \frac{\sqrt{3}a}{2\pi\sqrt{-1}} \log \frac{L_1}{|L_1|} + \frac{a}{2\sqrt{3}} \right)$$

with $L_1 = \sqrt{2}\ell_1 a + \sqrt{2}a/2 + \sqrt{2}\ell_2 a/2 - x_0$
 $+ \sqrt{-1}((\sqrt{6}\ell_2 a - \sqrt{6}a/3)/2 - y_0)$
for $x = \ell_1(a_1 - a_3) + \ell_2(a_2 - a_3) + a_1 - b \in \mathcal{B}^{(1)}$,

The third layer:

$$\left(\sqrt{2}\ell_1 a + \sqrt{2}a/2 + \sqrt{2}\ell_2 a/2, (\sqrt{6}\ell_2 a + 2\sqrt{6}a/3)/2, \right.$$

$$\left. \frac{\sqrt{3}a}{4\pi\sqrt{-1}} \log \frac{L_2}{|L_2|} + \frac{a}{\sqrt{3}} \right)$$

with $L_2 = \sqrt{2}\ell_1 a + \sqrt{2}a/2 + \sqrt{2}\ell_2 a/2 - x_0$
 $+ \sqrt{-1}((\sqrt{6}\ell_2 a - 2\sqrt{6}a/3)/2 - y_0)$
for $x = \ell_1(a_1 - a_3) + \ell_2(a_2 - a_3) + a_1 + a_2 - b \in \mathcal{B}^{(2)}$.

Recently the configurations of the dislocations are studied in terms of the ab-initio computations [Cl]; however, as mentioned above, the boundary condition is crucial in the study of dislocations. Since our description of the configuration is for the region far from the dislocation line, the configuration should obey the classical mechanics as the continuum theory of dislocation. Even for the ab-initio computations of the core structure of a dislocation, our results may provide data for their boundary conditions. Furthermore, recently crystal structures can be observed directly and are analyzed in terms of the number theory [ISCKI] as well. In a similar sense, our results might provide new viewpoints for the study of dislocations.

Furthermore, even if the thermal fluctuation is locally larger than the elastic energy, our study shows that the topological defect cannot be neglected, since the contour integral of the configurations of atoms along a circle around the dislocation line gives the topological invariance, which is described in Remark 2.4 and Proposition 2.6 mathematically. For real materials, we must consider other effects, e.g., various dislocations, bend of dislocation lines, etc.; however, some of the properties based on topological arguments must be preserved in the discrete description as mentioned in Sections 3 and 4. We note that the relation to the path space in Section 2 is robust, since the abelian covering is associated with the contours of certain integrals as in the case of Riemann surfaces [KMP].

In Section 5, we have obtained the strain or elastic energy of the screw dislocation.

I. In the computation, we have considered the spring model of the SC lattice by assuming that we have springs for a certain set of edges of the lattice graph. As in Lemma 5.1, the increase in length caused by the dislocation strongly depends on the direction: as (5.5) shows, it is of order one with respect to the height difference ϵ for the edges including the a_3 -direction, while it is of order two for the other edges. Note that the latter can be neglected in the approximate computation of the relevant energy.

This means that even if we add, for example, a spring for each edge

$$[(\ell_1, \ell_2, \ell_3), (\ell_1 + 1, \ell_2 + 1, \ell_3 + 1)]$$

etc., the energy basically remains the same as that given in Theorem 5.2.

II. For simplicity, let us suppose that the position of the dislocation line corresponds to $(x_0, y_0) = (0, 0)$. As we have investigated the elastic energy for the annulus region

$$R_{\rho, N} := \left\{ (x, y) \in \mathbb{E}^2 \mid \rho a < \sqrt{x^2 + y^2} < Na \right\}$$

of the dislocation for the discrete picture in Theorem 5.2, let us also consider its counterpart for the continuum picture. It is well-known that the strain energy $E_{\rho, N}^c$ of the screw dislocation in the annulus region per unit length along $(0, 0, 1)$ -direction, in continuum picture, is expressed by

$$E_{\rho, N}^c = \frac{a^2 G}{4\pi} \log N/\rho,$$

where G is the shear modulus and a appears as the length of the Burgers vector (see [HB, eq.(4.20)]). This is given by

$$\int_{R_{\rho, N}} \frac{1}{2} \frac{a^2 G}{(2\pi)^2} \frac{1}{x^2 + y^2} dx dy = \frac{a^2 G}{8\pi^2} \int_{\rho a}^{Na} \frac{1}{r^2} r dr \int_0^{2\pi} d\theta = \frac{a^2 G}{4\pi} \log N/\rho,$$

where the integrand comes from the elastic energy

$$\begin{aligned}
 & \left(\frac{1}{2\pi\sqrt{-1}} \frac{\partial}{\partial x} \log \frac{x + \sqrt{-1}y}{|x + \sqrt{-1}y|} \right)^2 + \left(\frac{1}{2\pi\sqrt{-1}} \frac{\partial}{\partial y} \log \frac{x + \sqrt{-1}y}{|x + \sqrt{-1}y|} \right)^2 \\
 = & -\frac{4}{(2\pi)^2} \left(\frac{\partial}{\partial z} \frac{1}{2} \log \frac{z}{\bar{z}} \right) \left(\frac{\partial}{\partial \bar{z}} \frac{1}{2} \log \frac{z}{\bar{z}} \right) \\
 = & \frac{1}{(2\pi)^2} \frac{1}{z\bar{z}} = \frac{1}{(2\pi)^2} \frac{1}{x^2 + y^2}
 \end{aligned}$$

for $z = x + \sqrt{-1}y$ (see [HB, LL, N]).

Note that the modulus G is directly connected to the spring constant k_d/a in our discrete model, since the integral for computing the strain energy $E_{\rho,N}^c$ in the continuum picture corresponds to the summation over lattice points in the region in the discrete picture, and each term is consistent with each other as shown by equation (5.8). More precisely, we have considered only a layer of length a to evaluate the energy $E_{\rho,N}(x_0, y_0)$ in our discrete model, whereas $E_{\rho,N}^c$ is for the unit length along the dislocation line. By putting $G = k_d/a$, $E_{\rho,N}(0, 0)/a$ corresponds to $E_{\rho,N}^c$; in fact, by dividing the energy by the square a^2 of the length of the Burgers vector, we have that

$$\lim_{a \rightarrow 0} (1/a) E_{\rho,N}(0, 0)/a^2 = \lim_{a \rightarrow 0} E_{\rho,N}^c/a^2$$

holds. This means that our spring model, in discrete picture, is consistent with the known dislocation theory in continuum picture, so that our model is plausible in such a sense. However, as mentioned in I, the correspondence between the spring constant k_d and the shear modulus G does depend on the choice of the edges for springs. If we employ additional edges with their own spring constants, then the resulting elastic energy may have a different constant, and thus the correspondence might be modified.

For $N \rightarrow \infty$, the above energy $E_{\rho,N}^c$ in continuum picture diverges. This should be compared with the discrete picture: the elastic energy $E_{\rho,N}(x_0, y_0)$ in Theorem 5.2 also diverges for $N \rightarrow \infty$ due to the property of the Epstein-Hurwitz zeta function [T].

III. As mentioned just before the definition of A_ρ in (5.6), our description shows that there is a criterion for the core region of a screw dislocation from a viewpoint of elastic energy.

IV. The investigation in Section 5 can also be applied to the case of the BCC lattice with the help of Proposition 4.14, although it might be complicated.

V. Finally, let us demonstrate an application of our model using the zeta function as follows. The total strain energy of two dislocations whose dislocation lines are parallel to each other and correspond to $\mathcal{S}_+ = \{(x_0, y_0)\}$ and $\mathcal{S}_- = \{(x_0, -y_0)\}$ with $y_0 \neq 0$, is

well-known in the continuum picture as follows:

$$\begin{aligned}
 & E_{\rho,N}^c(\mathcal{S}) \\
 (6.4) \quad &= C \int_{R'_{\rho,N}} \frac{1}{(x-x_0)^2 + (y-y_0)^2} dx dy + C \int_{R'_{\rho,N}} \frac{1}{(x-x_0)^2 + (y+y_0)^2} dx dy \\
 & \quad - 2C \int_{R'_{\rho,N}} \frac{(x-x_0)^2 + (y+y_0)(y-y_0)}{((x-x_0)^2 + (y-y_0)^2)((x-x_0)^2 + (y+y_0)^2)} dx dy,
 \end{aligned}$$

where $0 < \rho < N$, $\mathcal{S} = \mathcal{S}_+ \cup \mathcal{S}_-$, $R'_{\rho,N} := R_{\rho,N,(x_0,y_0)} \cap R_{\rho,N,(x_0,-y_0)}$, and

$$R_{\rho,N,(x_0,\pm y_0)} := \left\{ (x, y) \in \mathbb{E}^2 \mid \rho a < \sqrt{(x-x_0)^2 + (y \mp y_0)^2} < Na \right\}$$

(see [HB, N]). Then we can show that for $\rho a > 2|y_0|$, $E_{\rho,N}^c(\mathcal{S})$ is finite and it converges for $N \rightarrow \infty$ (see appendix).

It is important to show that this phenomenon occurs also for the discrete picture, or for the SC lattice. Let us evaluate the elastic energy in our model used in Section 5 for the double screw dislocation

$$\begin{aligned}
 \check{\sigma}_{z_0, \bar{z}_0}(\ell_1 a, \ell_2 a) &= \check{\sigma}_{\{z_0, \bar{z}_0\}, 1}(\ell_1 a, \ell_2 a) \\
 &= \frac{\ell_1 a - x_0 + \sqrt{-1}(\ell_2 a - y_0)}{|\ell_1 a - x_0 + \sqrt{-1}(\ell_2 a - y_0)|} \frac{\ell_1 a - x_0 - \sqrt{-1}(\ell_2 a + y_0)}{|\ell_1 a - x_0 - \sqrt{-1}(\ell_2 a + y_0)|},
 \end{aligned}$$

instead of $\check{\sigma}_{z_0}(\ell_1 a, \ell_2 a)$, where $z_0 = x_0 + \sqrt{-1}y_0$, $x_0, y_0 \in \mathbb{R}$. We concentrate ourselves on $\Delta_{\ell_1, \ell_2}^{d(i, \pm)}$ and $\epsilon_{\ell_1, \ell_2}^{(i)}$ which mainly contribute to the energy. We have

$$\begin{aligned} \Delta_{\ell_1, \ell_2}^{d(i, \pm)} &= \pm \frac{1}{\sqrt{2}} \epsilon_{\ell_1, \ell_2}^{(i)} + o\left(\max\left\{\frac{a}{\sqrt{(\ell_1 a - x_0)^2 + (\ell_2 a - y_0)^2}}, \right. \right. \\ &\quad \left. \left. \frac{a}{\sqrt{(\ell_1 a - x_0)^2 + (\ell_2 a + y_0)^2}}\right\}\right), \\ \epsilon_{\ell_1, \ell_2}^{(1)} &= \frac{a}{2\pi} \left(-\frac{a(\ell_2 a - y_0)}{(\ell_1 a - x_0)^2 + (\ell_2 a - y_0)^2} + \frac{a(\ell_2 a + y_0)}{(\ell_1 a - x_0)^2 + (\ell_2 a + y_0)^2} \right) \\ &\quad + o\left(\max\left\{\frac{a}{\sqrt{(\ell_1 a - x_0)^2 + (\ell_2 a - y_0)^2}}, \right. \right. \\ &\quad \left. \left. \frac{a}{\sqrt{(\ell_1 a - x_0)^2 + (\ell_2 a + y_0)^2}}\right\}\right), \\ \epsilon_{\ell_1, \ell_2}^{(2)} &= \frac{a}{2\pi} \left(-\frac{a(\ell_1 a - x_0)}{(\ell_1 a - x_0)^2 + (\ell_2 a - y_0)^2} + \frac{a(\ell_1 a - x_0)}{(\ell_1 a - x_0)^2 + (\ell_2 a + y_0)^2} \right) \\ &\quad + o\left(\max\left\{\frac{a}{\sqrt{(\ell_1 a - x_0)^2 + (\ell_2 a - y_0)^2}}, \right. \right. \\ &\quad \left. \left. \frac{a}{\sqrt{(\ell_1 a - x_0)^2 + (\ell_2 a + y_0)^2}}\right\}\right). \end{aligned}$$

Let us put $B'_{\rho, N} := B_{\rho, N, (x_0, y_0)} \cap B_{\rho, N, (x_0, -y_0)}$ for

$$B_{\rho, N, (x_0, \pm y_0)} := \left\{ (x, y) \in \mathbb{Z}^2 \mid \rho a < \sqrt{(ax - x_0)^2 + (ay \mp y_0)^2} < Na \right\}.$$

Then the elastic energy of the configuration for our \mathcal{S} is given by

$$\begin{aligned}
 & E_{\rho,N}(\mathcal{S}) \\
 := & \sum_{(\ell_1,\ell_2) \in B'_{\rho,N}} \frac{1}{2} k_d \left(\left(\Delta_{\ell_1,\ell_2}^{d(1,+)} \right)^2 + \left(\Delta_{\ell_1,\ell_2}^{d(2,+)} \right)^2 + \left(\Delta_{\ell_1,\ell_2}^{d(1,-)} \right)^2 + \left(\Delta_{\ell_1,\ell_2}^{d(2,-)} \right)^2 \right) \\
 = & k_d \sum_{(\ell_1,\ell_2) \in B'_{\rho,N}} \left(\frac{1}{2} (\epsilon_{\ell_1,\ell_2}^{(1)})^2 + \frac{1}{2} (\epsilon_{\ell_1,\ell_2}^{(2)})^2 \right) \\
 & + o \left(\max \left\{ \frac{a^2}{(\ell_1 a - x_0)^2 + (\ell_2 a - y_0)^2}, \frac{a^2}{(\ell_1 a - x_0)^2 + (\ell_2 a + y_0)^2} \right\} \right) \\
 = & \frac{1}{8\pi^2} k_d a^2 \sum_{(\ell_1,\ell_2) \in B'_{\rho,N}} \left(\frac{a^2}{(\ell_1 a - x_0)^2 + (\ell_2 a - y_0)^2} \right. \\
 & + \frac{a^2}{(\ell_1 a - x_0)^2 + (\ell_2 a + y_0)^2} \\
 & \left. - 2 \frac{a^2 ((\ell_1 a - x_0)^2 + (\ell_2 a + y_0)(\ell_2 a - y_0))}{((\ell_1 a - x_0)^2 + (\ell_2 a - y_0)^2)((\ell_1 a - x_0)^2 + (\ell_2 a + y_0)^2)} \right) \\
 & + o \left(\max \left\{ \frac{a^2}{(\ell_1 a - x_0)^2 + (\ell_2 a - y_0)^2}, \frac{a^2}{(\ell_1 a - x_0)^2 + (\ell_2 a + y_0)^2} \right\} \right).
 \end{aligned}$$

Let us assume that $\rho > 2|y_0|$. Then, using the property of the Epstein zeta function [T, Cor. 1.4.4], we can show that the energy $E_{\rho,N}(\mathcal{S})$ is finite even for $N \rightarrow \infty$ (see appendix).

This shows that the properties of zeta functions enable us to evaluate the discrete system in a rigorous manner. We believe that our investigation is necessary for clarifying discrete systems, e.g., in the framework of the classical statistical mechanics.

APPENDIX

In this appendix, we show that the total energy for the double screw dislocations discussed in Section 6 converges for $N \rightarrow \infty$ both in the continuum picture and in the discrete picture.

Lemma 6.1. *Suppose $\rho a > 2|y_0|$. Then, the strain energy $E_{\rho,N}^c(\mathcal{S})$ given in (6.4) for the region $R'_{\rho,N}$ in the continuum picture converges for $N \rightarrow \infty$.*

Proof. Note that the integrand is given as

$$\begin{aligned} & \frac{1}{(x-x_0)^2 + (y-y_0)^2} + \frac{1}{(x-x_0)^2 + (y+y_0)^2} \\ & - \frac{2((x-x_0)^2 + (y+y_0)(y-y_0))}{((x-x_0)^2 + (y-y_0)^2)((x-x_0)^2 + (y+y_0)^2)} \\ & = \frac{4y_0^2}{((x-x_0)^2 + (y-y_0)^2)((x-x_0)^2 + (y+y_0)^2)} \end{aligned}$$

and that $R'_{\rho,N} \subset R_{\rho',N,(x_0,0)}$ for some $\rho' > 0$ with $\rho'a > |y_0|$. Then, we have

$$\begin{aligned} & C^{-1}E_{\rho,N}^c(\mathcal{S}) \\ & \leq \int_{R_{\rho',N,(x_0,0)}} \frac{4y_0^2}{((x-x_0)^2 + (y-y_0)^2)((x-x_0)^2 + (y+y_0)^2)} dx dy \\ & =: E_{\mathcal{S},0}. \end{aligned}$$

We may assume that y_0 is positive. By using the polar coordinate (r, θ) centered at $(x_0, 0)$ such that $x = x_0 + r \cos \theta$ and $y = r \sin \theta$, we have

$$\begin{aligned} E_{\mathcal{S},0} & = \int_0^{2\pi} \int_{\rho'a}^{Na} \frac{4y_0^2 r}{(r^2 - 2y_0 r \sin \theta + y_0^2)(r^2 + 2y_0 r \sin \theta + y_0^2)} dr d\theta \\ & \leq \int_0^{2\pi} \int_{\rho'a}^{Na} \frac{4y_0^2 r}{(r - y_0)^4} dr d\theta \\ & = 8\pi y_0^2 \int_{\rho'a}^{Na} \left(\frac{1}{(r - y_0)^3} + \frac{y_0}{(r - y_0)^4} \right) dr \\ & = 8\pi y_0^2 \left(\frac{1}{2(\rho'a - y_0)^2} + \frac{y_0}{3(\rho'a - y_0)^3} - \frac{1}{2(Na - y_0)^2} - \frac{y_0}{3(Na - y_0)^3} \right) \\ & \rightarrow 8\pi y_0^2 \left(\frac{1}{2(\rho'a - y_0)^2} + \frac{y_0}{3(\rho'a - y_0)^3} \right) \end{aligned}$$

as $N \rightarrow \infty$, which means that $E_{\mathcal{S},0}$ does not diverge for $N \rightarrow \infty$. This completes the proof. \square

Lemma 6.2. *Suppose $\rho a > 2|y_0|$. Then, the elastic energy $E_{\rho,N}(\mathcal{S})$ for the region $B_{\rho,N}$ in the discrete picture converges for $N \rightarrow \infty$.*

Proof. Set

$$\begin{aligned} I &:= \frac{a^2}{(\ell_1 a - x_0)^2 + (\ell_2 a - y_0)^2} + \frac{a^2}{(\ell_1 a - x_0)^2 + (\ell_2 a + y_0)^2} \\ &\quad - 2 \frac{a^2((\ell_1 a - x_0)^2 + (\ell_2 a + y_0)(\ell_2 a - y_0))}{((\ell_1 a - x_0)^2 + (\ell_2 a - y_0)^2)((\ell_1 a - x_0)^2 + (\ell_2 a + y_0)^2)} \\ &= 4 \frac{a^2 y_0^2}{((\ell_1 a - x_0)^2 + (\ell_2 a - y_0)^2)((\ell_1 a - x_0)^2 + (\ell_2 a + y_0)^2)}. \end{aligned}$$

We may assume that $y_0 > 0$. Then, for $\ell_2 \geq 0$, we have $(\ell_2 a + y_0)^2 \geq (\ell_2 a - y_0)^2$ and

$$I \leq \frac{4a^2 y_0^2}{((\ell_1 a - x_0)^2 + (\ell_2 a - y_0)^2)^2},$$

whereas for $\ell_2 \leq 0$, we have $(\ell_2 a + y_0)^2 \leq (\ell_2 a - y_0)^2$ and

$$I \leq \frac{4a^2 y_0^2}{((\ell_1 a - x_0)^2 + (\ell_2 a + y_0)^2)^2}.$$

Furthermore, since for the Epstein zeta function, the value

$$\sum_{(\ell_1, \ell_2, \dots, \ell_n) \in \mathbb{Z}^n \setminus \{(0, 0, \dots, 0)\}} \frac{1}{(\ell_1^2 + \ell_2^2 + \dots + \ell_n^2)^{s/2}}$$

is finite for $s > n$ [T, Cor. 1.4.4], we see that the elastic energy $E_{\rho, N}(\mathcal{S})$ converges for $N \rightarrow \infty$. This completes the proof. \square

Note that in Lemma 6.2, we need the assumption $\rho > 2|y_0|$ in order to avoid the core regions around the dislocation centers.

Acknowledgements: The authors would like to express their sincere gratitude to all those who participated in the problem session ‘‘Mathematical description of disordered structures in crystal’’ in the Study Group Workshop 2015 held in Kyushu University and in the University of Tokyo during July 29–August 4, 2015 [O]. They are grateful to Professors Motoko Kotani, Takayuki Oda and Tatsuya Tate for helpful comments and to Professor Shun-ichi Amari for sending them his works [A1, A2]. The 2nd author has been supported in part by JSPS KAKENHI Grant Number 16K05187. The 4th author has been supported in part by JSPS KAKENHI Grant Number 15K13438. The second author thanks Professor Kenichi Tamano for critical discussions for an earlier version of this article. The authors also thank Professor Yohei Kashima and Professor Akihiro Nakatani for pointing out the analysis of a pair of dislocations. Thanks are also to the anonymous referees for critical suggestions and comments for the previous version, especially for the section for physicists, Remarks 4.3 and 4.6, and the expression (5.10) of the energy for the annulus region.

REFERENCES

- [A1] S. Amari, *On some primary structures of non-Riemannian plasticity theory*, RAAG Memoirs **3** (1962), 163–172.
- [A2] S. Amari, *A geometrical theory of moving dislocations and anelasticity*, RAAG Memoirs **4** (1968), 284–294.
- [BT] R. Bott and L.W. Tu, *Differential Forms in Algebraic Topology*, Graduate Texts in Mathematics, Vol. 82, Springer, 1982.
- [B] J.-L. Brylinski, *Loop Spaces, Characteristic Classes and Geometric Quantization*, Birkhäuser, 1993.
- [Ca] J.W.S. Cassels, *An Introduction to the Geometry of Numbers*, Springer, 1959.
- [Cl] E. Clouet, *Screw dislocation in zirconium: An ab initio study*, Phys. Rev. B **86** (2012) 144104.
- [CS] J.H. Conway and N.J.A. Sloane, *Sphere Packings, Lattices and Groups*, 3rd ed., Springer, 1999.
- [ES] J. Eells, Jr. and J.H. Sampson, *Harmonic mappings of Riemannian manifolds*, Amer. J. Math. **86** (1964), 109–160.
- [El] E. Elizalde, *On the zeta-function regularization of a two-dimensional series of Epstein-Hurwitz type*, J. Math. Phys. **31** (1990), 170–174.
- [Ep] P. Epstein, *Zur Theorie allgemeiner Zetafunktionen*, Math. Ann. **56** (1903), 615–644.
- [HB] D. Hull and D.J. Bacon, *Introduction to Dislocation*, 4th ed., Elsevier, 2011.
- [ISCKI] K. Inoue, M. Saito, C. Chen, M. Kotani, and Y. Ikuhara, *Mathematical analysis and STEM observations of arrangement of structural units in $\langle 001 \rangle$ symmetrical tilt grain boundaries*, Microscopy **65** (2016), 479–487.
- [I] T. Iwahori, *Goudou-henkan-gun-no-hanashi (Stories of Affine Transformation Groups)*, in Japanese, Gendai-sugakusha, 2000.
- [KE] A. Kadić and D.G.B. Edelen, *A Gauge Theory of Dislocations and Disclinations*, Springer, 1983.
- [Koh] T. Kohno, *Kesshou-gun (Crystal group)*, in Japanese, Kyouritsu, 2015.
- [KMP] J. Komeda, S. Matsutani and E. Previato, *The Riemann constant for a non-symmetric Weierstrass semigroup*, Arch. Math. **107** (2016), 499–509.
- [Kon] I. Kondo, *On the analytical and physical foundations of the theory of dislocations and yielding by the differential geometry of continua*, Int. J. Engng. Sci. **2** (1964) 219–251.
- [LL] L.D. Landau and E.M. Lifshitz, *Theory of Elasticity (Course of Theoretical Physics)*, Pergamon Press, 1970.
- [L] J.L. Lang, *Algebra*, Springer, 2004.
- [M] S. Matsutani, *Senkei-daisu-shuyu (Stories in Linear Algebra)*, in Japanese, Gendai-sugakusha, 2013.
- [N] F.R.N. Nabarro, *Theory of Crystal Dislocations*, Oxford Univ. Press, 1967.
- [O] K. Okada, K. Fujisawa, T. Shirai, M. Wakayama, H. Waki, P. Broadbridge and M. Yamamoto (editors), *Study Group Workshop 2015, Abstract, Lecture & Report*, MI Lecture Notes, Vol. 66, 2015.
- [S] T. Sunada, *Crystals that nature might miss creating*, Notices Amer. Math. Soc. **55** (2008), 208–215.
- [T] A. Terras, *Harmonic Analysis on Symmetric Spaces – Higher Rank Spaces, Positive Definite Matrix Space and Generalizations*, Springer, 2016.
- [U] K. Uhlenbeck, *Harmonic maps into Lie groups: classical solutions of the chiral model*, J. Differential Geom. **30** (1989), 1–50.

H. Hamada:

National Institute of Technology, Sasebo College,
1-1 OkiShin-machi, Sasebo, Nagasaki, 857-1193, JAPAN

S. Matsutani:

National Institute of Technology, Sasebo College,
1-1 OkiShin-machi, Sasebo, Nagasaki, 857-1193, JAPAN

J. Nakagawa:

Mathematical Science & Technology Research Labs,
Nippon Steel & Sumitomo Metal Corporation,
20-1 Shintomi, Futtsu, Chiba, 293-8511, JAPAN

O. Saeki:

Institute of Mathematics for Industry,
Kyushu University,
744 Motooka, Nishi-ku, Fukuoka 819-0395, JAPAN

M. Uesaka:

Graduate School of Mathematical Sciences,
The University of Tokyo,
3-8-1 Komaba, Meguro-ku, Tokyo, 153-8914, JAPAN